Targeted Anatomical and Functional Identification of Antinociceptive and Pronociceptive Serotonergic Neurons that Project to the Spinal Dorsal Horn

Abbreviated title: Descending Serotonergic Projection Neurons

Robert P. Ganley[1], Marilia Sousa[1], Kira Werder[1], Tugce Öztürk[2], Hendrik Wildner[1] & Hanns Ulrich Zeilhofer[1,2]

[1]Institute for Pharmacology and Toxicology, University of Zürich, CH-8057 Zürich, Switzerland
[2]Institute of Pharmaceutical Sciences, Swiss Federal Institute of Technology Zürich, CH-8090, Zürich, Switzerland

Corresponding authors: robert.ganley@pharma.uzh.ch, zeilhofer@pharma.uzh.ch

Pages: 37
Figures: 7
Tables: 7
Number of words
Abstract: 205
Introduction: 600
Discussion: 1619

Conflict of interest: none

Acknowledgements: We are grateful for funding provided by grants from the Swiss National Science Foundation (grant number 310030_197888) and by the clinical research priority programme (CRPP) “Pain – from phenotypes to mechanisms” of the Faculty of Medicine, University of Zurich, to HUZ, and a grant from the Olga Mayenfisch Stiftung to HW. We thank Louis Scheurer, Katharina Struckmeyer-Fichtel, and Isabelle Kellenberger for technical support.

Abstract

Spinally-projecting serotonergic neurons play a key role in controlling pain sensitivity and can either increase or decrease nociception depending on physiological context. It is currently unknown how serotonergic neurons mediate these opposing effects. Utilizing virus-based strategies, we identified two anatomically separated populations of serotonergic hindbrain neurons located in the lateral paragigantocellularis (LPGi) and the medial hindbrain, which respectively innervate the superficial and deep spinal dorsal horn and have contrasting effects on pain perception. Our tracing experiments revealed an unexpected high selectivity of serotonergic neurons of the LPGi for transduction with spinally injected AAV2retro vectors while medial hindbrain serotonergic neurons were largely resistant to AAV2retro transduction. Taking advantage of this selectivity, we employed intersectional chemogenetic approaches to demonstrate that activation of the LPGi serotonergic projections decreases thermal sensitivity, whereas activation of medial serotonergic neurons increases sensitivity to mechanical von Frey stimulation. Together these results suggest that there are functionally distinct classes of serotonergic hindbrain neurons that differ in their anatomical location in the hindbrain, their postsynaptic targets in the spinal cord, and impact on nociceptive sensitivity. At least the LPGi neurons give rise to rather global and bilateral projections throughout the rostrocaudal extent of the spinal cord suggesting that they contribute to widespread systemic pain control.

Introduction

Descending pain control is a critical endogenous mechanism of pain modulation that is required for the survival [37], and allows an organism to respond in an appropriate context-dependent manner to external threats. Key brain structures involved in this system were discovered through stimulation-produced analgesia experiments and include the periaqueductal grey matter (PAG) and the rostroventromedial medulla (RVM) of the hindbrain [9]. This descending system acts to inhibit the flow of nociceptive information through the spinal dorsal horn and requires descending tracts within the dorsolateral funiculus to mediate its effects [8; 10]. The RVM is also required for maintaining some chronic pain states through a process of descending facilitation [42; 60], indicating that this area has a bidirectional control over pain sensitivity. Both descending inhibition and facilitation will ultimately require the activation of descending tracts to modulate the neuronal activity within the dorsal horn. To understand the precise neuronal circuitry and transmitter systems underlying descending pain inhibition and facilitation, an understanding of the different projection neurons from the RVM to the spinal cord is needed.

Monoamines are important neurotransmitters involved in descending pain control, with serotonin (5-HT) being able to inhibit nociception when injected intrathecally [50]. Spinal 5-HT is also known to mediate certain forms of endogenous pain suppression, such as stress-induced analgesia [58], but is also required to maintain chronic pain in rodent models of nerve injury [52]. This pain facilitation in pre-clinical neuropathy models is thought to be a result of reduced tonic diffuse noxious inhibitory controls, due to increased spinal 5-HT_3 receptor activation [4; 6]. The variety and abundance of 5-HT receptors within the spinal dorsal horn likely explains, at least in part, why these multiple effects are observed [7]. Clearly, spinal 5-HT and the serotonergic projections to this region have a complex and bidirectional control over pain control that requires further study.

Functional studies of specific descending projections have been facilitated by the development of viral retrograde tracers, such as AAV2retro and canine adenoviruses [23; 28; 46]. However, it has been reported that the AAV2retro serotype, may not infect serotonergic hindbrain neurons as efficiently as other descending projections [46; 51]. Further, despite the dense serotonergic innervation of the spinal dorsal horn, studies employing monosynaptic neuronal circuit tracing from dorsal horn neurons with modified rabies viruses rarely found labeled hindbrain serotonergic neurons [23; 34]. This is surprising since both descending serotonergic neurons and dorsal horn interneurons are known to strongly influence nociception, and it is possible that these rabies virus-based tracers fail to detect functional connections between serotonergic neurons and starter populations within the spinal cord. Together these reports would suggest that descending serotonergic projections of the hindbrain are particularly challenging to study using the currently available tools.

In an attempt to address this discrepancy, we compared the labeling efficiency of a range of viral and non-viral tracers. Specifically, we examined the susceptibility of serotonergic hindbrain neurons to retrograde spinal transduction by AAV2retro serotype vectors [46]. Additionally, we traced serotonergic neurons of the hindbrain with modified rabies viruses and tested whether they could be labelled from dorsal horn neuron starter populations with monosynaptic rabies tracing. To allow functional interrogation of descending serotonergic neurons, we assessed the specificity of the TPH2::Cre mouse line and used this together with the preferential transduction efficiency of AAV2retro to develop an intersectional system that allowed selective labelling and manipulation of serotonergic neurons in the lateral paragigantocellularis (LPGi), or the medial nucleus raphe magnus (NRM). We find that the lateral and medial serotonergic neurons of the RVM are distinct in terms of their anatomical organization, resistance to AAV2retro transduction, and influence on acute nociception.

Methods

Animals

Mice of either sex aged between 6-12 weeks were used for experiments. Permission to perform these experiments was obtained from the Veterinäramt des Kantons Zürich (154/2018 and 063/2016). The various transgenic mouse lines used in this study are listed in table 1.

Surgeries

The dorsal horn of the lumbar spinal cord was injected in a similar manner to previous studies [24; 27]. Briefly, anesthesia of mice was induced with 5% Isoflurane in an induction chamber. Mice were then transferred to a stereotaxic injection setup and anesthesia was maintained with 1-3% Isoflurane delivered through a face mask. Body temperature was maintained using a heated mat placed beneath the animal. Vitamin A cream was applied to the eyes to prevent corneal drying during the operation and buprenorphine (0.1-0.2 mg/kg) was injected subcutaneously prior to the operation. The back of the animal was shaved, and the skin was scrubbed with Betadine solution. Once dried, a midline incision was made above the vertebral column to expose the T13 vertebra, which was clamped using a pair of spinal adaptors to isolate movements from the animal's breathing. A borehole was made in the center of the left-hand side of the clamped vertebra and viruses, 1% cholera toxin b (CTb), or 4% fluorogold were injected into the dorsal horn at a depth of 300 μm below the spinal surface approximately 500 μm left of the central artery. For most injections, 3 x 300 nl virus solution was injected along the rostrocaudal extent of the spinal cord at an infusion rate of 50 nl/min. For monosynaptic tracing experiments, the rabies virus was injected 2 x 500 nl at either side of the T13 vertebra in the same region as the injection of helper virus, which was injected two weeks previously. Experiments involving intraspinal injection of Fluorogold were abandoned shortly after animal recovery due to adverse effects, which exceeded the

tolerance allowed according to the permission granted for animal experimentation ((154/2018 and 063/2016). For a list of the retrograde tracers and viruses used in this study, please refer to tables 2 and 3.

For injections into the hindbrain, animals were prepared for surgery in a similar manner to the spinal cord injections. The head was fixed in position using ear bars mounted on the stereotaxic frame (Kopf instruments). Coordinates were chosen based on the hindbrain location of the TPH2::Cre neurons retrogradely labelled from the spinal cord with reference to a mouse brain atlas (-6, +/-0.5, 5.9 relative to bregma, 1 μl per injection site, infusion rate 50 nl/min). injections into the midline nucleus raphe magnus were made at coordinates -6, 0, 5.9 and a volume of 300nl was chosen to limit the transgene expression to the medial serotonergic neurons. The movement of the frame was achieved using motorized axes controlled by a computer interface, which was also used to select the injection target (Neurostar). This same software was used to adjust the injection target for tilt and scaling, by adjusting the mouse brain atlas relative to four points on the surface of the skull (Bregma, Lambda, 2 mm to the right of the midline, and 2 mm to the left of the midline).

General features of tissue preparation and immunohistochemistry

Animals were perfusion fixed with freshly depolymerized 4% paraformaldehyde (room temperature, dissolved in 0.1 M PB, adjusted to pH 7.4) following a brief rinse of the mouse circulatory system with 0.1 M PB. Nervous tissues were quickly dissected and post-fixed in the same fixative for two hours at 4˚C. After post-fixation, tissues were rinsed 3 times with 0.1 M PB and placed in 30% sucrose solution (w/v dissolved in 0.1 M PB) for 24-72 hours for cryoprotection. Tissues were rinsed with 0.1 M PB before being embedded in NEG-50 mounting medium and were either cut at 60 μm on a sliding blade microtome (Hyrax KS 34, histocam AG) and stored as free-floating sections, or were cut at 30 μm using a cryostat (Hyrax 60, histocam AG) and were mounted directly onto microscope slides (Superfrost Plus, Thermoscientific).

Free floating sections were processed immediately for tissue staining or were stored in antifreeze medium (50 mM sodium phosphate buffer, 30% ethylene glycol, 15% glucose, and sodium azide (200 mg/L) at -20°C until required. Antifreeze medium was removed by rinsing sections three times in 0.1 M PB before further processing. Sections were rinsed in 50% ethanol for 30 minutes at room temperature, followed by three rinses in PBS with added salt (8 g NaCl per liter of PBS). Alternatively, slides were prepared by mounting frozen sections directly onto superfrost slides. These were either used immediately for immunostaining or stored at -80°C until further use. Before immunostaining, excess NEG50 freezing medium was removed by rinsing in 0.1 M PB for one hour at room temperature. A hydrophobic barrier was drawn around the sections using a fat pen, and immunoreactions were performed on the slides.

All primary antibodies and dilutions used in this study are included in table 4. Primary antibodies were diluted in a PBS solution containing extra salt (8g NaCl per liter), 0.3% v/v Triton-X, and 10% v/v normal donkey serum. Secondary antibodies were diluted in a similar solution, but without the 10% normal donkey serum (Table 4). Sections or slides were incubated in primary antibodies for 24 – 72 hours at 4°C, and these were revealed by incubation in secondary antibodies overnight at 4°C. Following immunostaining, sections or slides were rinsed three times for 10 minutes each in PBS solution containing extra salt before being mounted in Dako anti-fade medium.

Rabies virus tracing experiments

Rabies virus tracing experiments used either the SAD-G pseudotyped or EnvA pseudotyped RabΔG-GFP viruses, which are deficient in the SAD-glycoprotein required for transsynaptic spread and contain eGFP for identification of infected cells [54; 55]. Rabies viruses pseudotyped with the SAD-G glycoprotein can directly infect most, but not all, types of neurons [2; 54]. The rabies viruses that are pseudotyped with the EnvA glycoprotein are only able to infect cells through binding to the TVA receptor. Therefore, the restricted expression

of the TVA receptor to certain cell types allows the selective infection of those neurons with EnvA pseudotyped rabies viruses [55]. For monosynaptic tracing experiments, the helper virus containing the rabies glycoprotein was injected two weeks prior to rabies virus injection to enable transsynaptic spread.

Animals were perfused 5 or 7 days after dorsal horn injection of rabies viruses. Hindbrain sections from rabies virus injected tissue were cut at 30 μm and mounted directly onto microscope slides. Tissues were immunostained for eGFP and TPH2 to determine the proportion of labelled hindbrain neurons that contained detectable TPH2.

Image acquisition and analysis

For quantification of retrogradely labelled cells in the hindbrain, image stacks were acquired at 5 μm z-spacing using a Zeiss lsm 800 confocal microscope with Zen blue software. Confocal scans were made using 488, 561 and 640 nm lasers and the pinhole was set to 1 Airy Unit for reliable optical sectioning. Care was taken to acquire image stacks up to a depth where there was clear immunoreactivity of all antigens to avoid false negatives during quantification due to antibody penetration. Within each experiment, all acquisition settings were kept constant, and images were analyzed with FIJI using the cell counter plugin.

Alternatively, an automated cell quantification pipeline was designed in CellProfiler to count retrogradely labelled neurons in the RVM. We noticed that many large neurons within the RVM contained NeuN immunoreactivity that was present in more than one image in the image stacks (5 μm z-spacing). Automated counting of all images within each z-stack would lead to double counting a large proportion of cells present on multiple images within the image stack. However, if only one image was analyzed per image stack, numerous cells would be excluded from the analysis. Therefore, the acquired z-stacks were processed into either one to two orthogonal projections from 2 images to reduce the double counting of cells whilst ensuring the counting of most visible cells within each stack. One sample projection

was then counted manually using the cell counter plugin of ImageJ, to serve as a guide in the development of the CellProfiler pipeline. All orthogonal projections were processed using the same CellProfiler pipeline with set parameters to ensure consistent data collection.

The images were loaded into this CellProfiler pipeline and the three channels (CTb, eGFP and NeuN) were separated from each other. NeuN- and CTb-stained neurons were identified as primary objects using the two-class Otsu method as a global thresholding strategy, whilst eGFP-containing objects were identified using the adaptive thresholding strategy (with an adaptive window of 50 pixels). NeuN stained cells were distinguished from the background based on their intensity, whereas the method used for detecting CTb and eGFP positive cells was based on their shape. The NeuN objects were converted into a binary (black & white) image and the coexpression of eGFP or CTb was assessed. The object counts of eGFP/NeuN, CTb/NeuN, eGFP/CTb/NeuN and NeuN positive objects were then extracted and exported to a spreadsheet.

To quantify the cells labelled from rabies tracing experiments that were serotonergic, cell bodies were identified in the ventral hindbrain that were labelled with eGFP. These were scanned on a Zeiss 710 LSM confocal microscope, either as a short stack through the cell body, or as a single optical section through the center of the neuron. Scan settings were determined by the fluorescent intensity of the surrounding TPH2 immunoreactive regions in the nucleus raphe magnus (NRM) and lateral paragigantocellularis (LPGi) and were kept consistent for all experiments. Cell identities were catalogued and TPH2 immunoreactivity was determined for all sampled cells.

Slice preparation and electrophysiology

Hindbrain slices were prepared from TPH2::Cre animals that had received a bilateral injection of AAV9.flex.tdTomato into the ventral hindbrain. Animals were aged 3-6 weeks at the time of injection and were prepared for electrophysiological recordings 1-2 weeks later. Slices were prepared in a similar manner to previous studies [38; 59]. Animals were

decapitated and the brain was rapidly dissected and placed in ice cold oxygenated dissection solution (containing in mM (65 NaCl, 105 sucrose, 2.5 KCl, 1.25 NaH_2PO_4, 25 $NaHCO_3$, 25 glucose, 0.5 $CaCl_2$, 7 $MgCl_2$). The hindbrain was isolated, glued to a block of 2% agarose and installed in a slicing chamber. Transverse slices of hindbrain were cut at 250 μm on a vibrating blade microtome (D.S.K microsclicer DTK1000), which were allowed to recover for at least 30min in oxygenated aCSF at 34°C prior to recording, containing (in mM) 120 NaCl, 26 $NaHCO_3$, 1.25 NaH_2PO_4, 2.5 KCl, 5 HEPES, 14.6 glucose, 2 $CaCl_2$, 1 $MgCl_2$), pH 7.35 - 7.40, osmolarity 305 - 315 mOsm.

During recording, slices were perfused with aCSF at a flow rate of 2-3 ml/min. Targeted recordings were taken from tdTomato-expressing neurons using glass microelectrodes filled with a K-gluconate internal solution (containing 130 K-Gluconate, 5 NaCl, 1 EGTA, 10 HEPES, 5 Mg-ATP, 0.5 Na-GTP, 2 biocytin). Whole-cell recordings were acquired using a HEKA EPC10 amplifier with Patchmaster software at a sampling frequency of 20 kHz (HEKA Elektronik). A biophysical characterization of passive and active membrane properties was performed in current and voltage clamp modes, and the access resistance was monitored between recordings using a 10mV voltage step protocol. Data were excluded if the access resistance changed >30% during recording.

The relative position of the recorded/labelled neurons in each slice was noted, and slices were fixed overnight in 4% PFA at 4°C at the end of each experiment. Slices were immunoreacted with primary antibodies against tdTOM and TPH2, which were revealed the next day with secondary antibodies conjugated to Cy3 or Alexa 647. Biocytin was revealed with Avidin-Alexa A488 and the position of the filled neurons was assigned to the NRM or the LPGi, which could be determined based on the pattern of TPH2 immunoreactivity in the slice. Cells located outside of these two regions were not analyzed further.

Behavioral assays

For specific DREADD-mediated activation of descending serotonergic pathways, an intersectional approach was used for labelling the lateral hindbrain neurons whereas direct labelling was used to label the medial neurons. TPH2::Cre mice received an intraspinal injection of AAV2retro.flex.FLPo.BFP, and one week later received bilateral injections into the ventral hindbrain with AAV1.FRT.hM3Dq.mCherry. Behavioral tests were performed after 10 days incubation time to allow the expression of the viral transgene. Before experiments mice were acclimatized to the behavioral setup for one hour. For the Hargreaves plantar, cold plantar, electronic von Frey, and Rotarod assays, six measurements were taken for each time point and an average of these was reported. All measurements were taken from both hindlimbs of all animals. Alternatively, serotonergic neurons in the medial hindbrain were labelled by injection of AAV8.hsyn.flex.hM3Dq into the NRM (injection coordinates -6, 0, 5.9) and the same behavioral tests were performed with the same experimental design.

Hargreaves

Sensitivity to heat stimuli was assessed with the Hargreaves plantar assay (IITC). Mice were placed on a pre-heated transparent platform set to a temperature of 30°C, and the withdrawal latencies were recorded using a timed infrared heat source. A resting intensity of 5% and an active intensity of 20% was used for stimulations, and a maximum cutoff time of 32 s was set to avoid tissue damage.

Cold plantar assay

Mice were placed on a 5 mm borosilicate glass platform and were stimulated from beneath with dry ice pellets. The time taken to withdraw the paw was measured using a stopclock and a maximum stimulation time of 20 s was used to avoid tissue damage.

von Frey

Von Frey thresholds were measured using an electronic von Frey algesiometer (IITC). Animals were adapted on a mesh surface, and the plantar surface of each paw was stimulated with a bendable plastic filament attached to a pressure sensitive probe. Pressure was applied to the plantar surface in a linear manner until the animal withdrew its paw, and the maximum pressure (the pressure at which the animal withdrew) was displayed on the device.

Rotarod

Sensorimotor coordination was evaluated using an accelerating rotarod, and the time taken for animals to fall from the rotating barrel was recorded. The barrel rotated from 4 - 40rpm over a period of 300s, and increased speed constantly throughout each experiment. Values were discarded if the animal jumped from the barrel, and if the animal jumped in >50% of trials for a given time point these data were discarded from the experiment. Two training sessions were given for all animals prior to the experiment being started to ensure a stable performance in the absence of treatment.

Drug application

For DREADD activation experiments, clozapine-N-oxide (CNO, 2 mg/kg, Enzo life sciences, product number BML-NS105-0025) or vehicle controls were injected intraperitoneally, with the experimenter being blinded to the injected substance. Animals were tested directly before and 1-3 hours following i.p. injection. Stock CNO was dissolved in DMSO at 100 mg/ml and kept at room temperature, which was diluted 1:500 in sterile filtered saline immediately prior to injection with the volume of injected substance being 10 μl/g.

Experimental design and statistical tests

All behavioral assays were performed twice on each animal so that they received an intraperitoneal injection of CNO on one day and Vehicle injection on the other, with the experimenter being blinded to the treatment. Response latencies and thresholds following CNO and Vehicle were compared using a repeated measures one-way ANOVA, a normal distribution was assumed for response latencies and thresholds and a Bonferroni post-hoc test was used to compare the mean withdrawal latencies and thresholds between CNO and vehicle treated groups before and 1-3 hours after injection. Statistical significance was taken as $P < 0.05$.

To compare membrane properties between medial and lateral serotonergic neurons, a normal distribution in values was assumed and an unpaired two-tailed t-test was used to test for differences.

Data collection, storage, and presentation

Data obtained from the quantification of images were collected and processed in Microsoft Excel and were presented using GraphPad Prism 5. All datapoints on graphs represent either a number or percentage of cells counted per animal, or as a response for each animal in behavioral assays. Representative images were produced in Affinity Photo and were annotated and arranged into figures in Affinity Designer. Raw data for these experiments are available on reasonable request and are located on the internal servers of the Institute for Pharmacology and Toxicology, University of Zürich.

Results

Serotonergic hindbrain neurons are rarely infected using monosynaptic rabies tracing from the dorsal horn

To explore which viral tools can be used to study descending serotonergic circuits, we started with intraspinal injection of modified rabies viruses. Monosynaptic rabies tracing is a commonly used technique for tracing neuronal circuits from genetically defined populations of neurons and provides useful information regarding the presynaptic inputs to a neuronal population. [55]. However, in the case of serotonergic neurons, the results of previous studies have demonstrated that very few neurons of the hindbrain are traced from dorsal horn starter populations, despite the dense serotonergic innervation of the superficial dorsal horn and the important role of serotonin in pain modulation [23; 34]. This suggests that serotonergic neurons are either traced with only limited efficacy, or that there is highly specific serotonergic innervation of some spinal neuron populations but not others.

To test whether serotonergic hindbrain neurons are resistant to rabies virus infection, we injected a rabies virus, whose genome lacked the glycoprotein-encoding sequence but was pseudotyped with the SAD glycoprotein (SAD.RabiesΔG-eGFP (SAD-G)), into the spinal dorsal horn (Figure 1A). This virus can directly infect most neurons but cannot be propagated beyond the initially infected neurons due to the lack of the rabies glycoprotein required for transsynaptic spread [2; 54]. Five days after injection of SAD.rabΔG-eGFP (SAD-G), 44% of the labelled hindbrain neurons contained detectable TPH2 immunoreactivity (Figure 1B and C). Notably, the percentage of labeled neurons dropped to only 12% of labelled hindbrain neurons at day 7 post injection (Figure 1C). This reduction may be a result of rabies virus toxicity, which could lead to a downregulation of cytoplasmic enzymes such as TPH2 to undetectable levels, and hence an underestimation of labelled serotonergic neurons. For this reason, we used a 5-day survival time for all subsequent experiments involving rabies viruses.

To determine whether serotonergic hindbrain neurons could be traced transsynaptically from the spinal dorsal horn, we used Hoxb8-Cre mice to define a broad starter population of spinal cord neurons. During development, Hoxb8-Cre is expressed transiently in almost all spinal neurons and astrocytes caudal to C4. It can be used to define a starter population that includes virtually all dorsal horn neurons [56]. We used Hoxb8-Cre; ROSA^{TVA} mice to induce stable expression of TVA in most dorsal horn neurons during development, enabling their infection in the adult with EnvA pseudotyped rabies viruses (SAD.Rabies∆G-GFP (EnvA)). To allow transsynaptic spread from the starter population, a helper virus containing mCherry and rabies glycoprotein was injected two weeks prior to injection of SAD.Rabies∆G-GFP (EnvA) (Figure 1D).

Five days after rabies virus injection, neurons in the ventral hindbrain labelled with eGFP were assessed for TPH2 expression by immunostaining. On average, the number of eGFP-labelled hindbrain neurons counted per animal was similar between direct and transsynaptic tracing from the spinal cord (8.3 and 8.25 respectively) We only observed coexpression of eGFP and TPH2 once in a total of 33 inspected neurons, corresponding to 3% of our total sample (Figure 1E and F). A summary of all rabies virus tracing experiments can be found in table 5. In the hindbrain, we never observed colocalization of mCherry and eGFP, suggesting that all eGFP-expressing neurons in the hindbrain were transsynaptically traced from the dorsal horn. Together these data demonstrate that although TPH2-expressing hindbrain neurons can be directly infected with modified rabies viruses, they are largely underrepresented with monosynaptic tracing from the dorsal horn. This may partly explain their absence from many of the circuit tracing studies that have used this approach.

Spinal injection of AAV2retro serotype vectors preferentially transduce TPH2-containing projection neurons in the lateral hindbrain

Next, we tested AAV vectors have been developed to permit the efficient retrograde labelling of projection neurons via their axon terminals [46]. However, it is debatable whether these

vectors are capable of transducing serotonergic neurons that project to the spinal cord [51]. To test this, we used AAV2retro serotype vectors to retrogradely label hindbrain neurons that project to the spinal cord to assess their ability to transduce serotonergic projection neurons (Figure 2A). Following intraspinal injection of AAV2retro.GFP, many transduced neurons were labelled within the RVM (Figure 2B). When we inspected the location of neurons that expressed both TPH2 and eGFP, we found that the majority of these cells were located lateral to the midline (Figure 2B). Quantification of the location of the eGFP-labelled TPH2-expressing neurons indicated that 74% were located in the lateral paragigantocellularis (LPGi) both ipsilateral and contralateral to the spinal cord injection site (left hand side). In agreement with [51], far fewer eGFP+TPH2+ neurons were found within the midline nucleus raphe magnus (NRM) (23/100 neurons in NRM, 3 - 12 (n=3 animals) (Figure 2C). However, most non-serotonergic projection neurons (eGFP+ TPH2-) were found close to the midline of the ventral hindbrain (412/439 neurons in midline, 102 - 193 (n=3 animals) (Figure 2B)

There is increasing evidence to suggest that some projections are resistant to retrograde transduction with AAV2retro vectors, and comparisons with independent tracing methods are required to demonstrate this resistance [24; 46]. To study the anatomical organization of serotonergic pathways using a non-viral method, we used Cholera toxin b subunit (CTb) retrograde tracing and compared the hindbrain labelling with our AAV2retro tracing experiments (Figure 2D).

Strikingly, many CTb-labeled TPH2-expressing hindbrain neurons were found in the midline NRM, although CTb-containing TPH2-expressing neurons were also found in the LPGi (Figure 2E). To directly test whether there were differences in labelling efficiency between AAV2retro and CTb-based tracing methods, AAV2retro.GFP and CTb were co-injected into the spinal dorsal horn (Figure 2F). In total more neurons in the ventral hindbrain were retrogradely labelled from the dorsal horn with CTb than AAV2retro.eGFP (Figure 2G and H) When only TPH2-expressing retrogradely labelled neurons were examined, a much lower

percentage of neurons was labelled with AAV2retro.GFP relative to the overall population of traced neurons (Figure 2H). However, when the retrogradely labelled TPH2+ neurons were divided into separate areas, it was apparent that a lower percentage of neurons in the NRM were labelled with eGFP compared to the LPGi (Figure 2H) whereas the proportion of serotonergic neurons in the LPGi labelled with AAV2retro, CTb, and both AAV2retro and CTb were similar to the general population of retrogradely labelled hindbrain neurons (Figure 2H and I). Therefore, we conclude that the reduced labelling of hindbrain serotonergic neurons with AAV2retro was due to a resistance of midline serotonergic neurons to AAV2retro-mediated transduction. In contrast, laterally located serotonergic neurons were highly susceptible to transsynaptic transduction with AAV2retro. A summary of these data can be found in table 6.

Descending serotonergic projection neurons of the LPGi can be preferentially labelled using AAV2retro vectors and TPH2::Cre mouse line

In order to study descending serotonergic neurons functionally, we must first identify a suitable method to specifically influence those neurons. TPH2-containing neurons of the LPGi were susceptible to retrograde transduction by AAV2retro in contrast to other serotonergic nuclei of the hindbrain (Figure 2), which would permit selective transduction of these neurons using AAV2retro. Further, mouse lines expressing Cre recombinase within defined neuronal populations have been widely and successfully used to functionally study a variety of spinal neuron subtypes [22; 25; 29; 39]. We therefore assessed the reliability of the TPH2::Cre mouse line as a marker of serotonergic neurons and a potential tool to gain genetic access to these cells. To determine whether the Cre expression in this mouse line was specific to serotonergic neurons that project to the spinal cord, we injected the lumbar dorsal horn of TPH2::Cre mice with an AAV2retro serotype vector containing a Cre-dependent eGFP construct (Figure 3A). This resulted in TPH2-expressing neurons of the hindbrain being labelled with eGFP, particularly in the LPGi (Figure 2B). In addition, many

neurons were labelled in the ipsilateral DRG (Figure 2C). We observed a similar pattern in cell location as in the AAV2retro.eGFP labelling experiments (Figure 2B and 3C), with 72% of eGFP neurons being present bilaterally in the LPGi (Figure 3D). Furthermore, 77.5% of all neurons labelled with AAV2retro.flex.eGFP contained detectable levels of TPH2 (Figure 3E). Therefore, among the hindbrain neurons that project to the spinal dorsal horn TPH2::Cre is expressed specifically in serotonergic neurons, but may also expressed in other neurons of the nervous system, including a subset of DRG neurons.

To specifically manipulate spinally-projecting serotonergic neurons without influencing other neuronal populations, such as those in the DRG, we used an intersectional strategy to induce reporter expression in spinally-projecting TPH2::Cre neurons of the hindbrain (Figure 3F). This strategy utilized AAV2retro serotype vectors containing a Cre-dependent optimized flippase (FLPo), which, when injected intraspinally, results in FLPo expression in Cre-expressing neurons that project to the dorsal horn. The AAV2retro serotype would also enable expression restricted to laterally located serotonin-expressing neurons. This construct also contained the coding sequence for mCherry, allowing these transduced cells to be visualized (AAV2retro.flex.FLPo.mCherry). The hindbrain was injected one week later with an AAV containing a flippase-dependent eGFP viral vector (AAV9.FRT.eGFP), to capture the neurons that were transduced from the spinal cord with AAV2retro (Figure 3F and G). This approach allowed the quantification of the intersectionally labelled serotonergic neurons (mCherry- and eGFP-expressing), relative to the population of directly labelled neurons from the spinal dorsal horn (mCherry-expressing). Therefore, the accuracy of the hindbrain injections and the proportion of the descending projection neurons captured within the injection site could be determined.

Different brain injection coordinates were tested to optimize the proportion of spinally-projecting TPH2::Cre neurons that were captured with the stereotaxic brain injection. Bilateral injections of AAV9.FRT.eGFP (-6, ±0.5, -5.9 relative to Bregma) was the most

efficient in terms of mCherry+eGFP+ neurons labelled in the hindbrain (Figure 3F and G). With this approach, we labelled 80.6% of all retrogradely transduced neurons with eGFP with the remaining 19.4% containing mCherry only, indicating that most retrogradely transduced neurons are labelled using this strategy. Additionally, this proportion was similar between the different areas containing retrogradely-labelled serotonergic neurons (LPGi = 80.6%, NRM = 78.3%, other = 82.4%, labelled neurons containing eGFP), suggesting that the injection sites encompass most regions containing AAV2retro-labelled serotonergic projection neurons. Some cells only contained eGFP without detectable mCherry staining, either due to non-specific recombination of the FRT sites or low to undetectable levels of mCherry present in these neurons. We found that a smaller proportion of eGFP-only neurons were present in the LPGi compared to the NRM (4.6% versus 16.9% respectively, Figure 3H). We concluded that this intersectional strategy is suitable for the specific manipulation of serotonergic hindbrain neurons that project to the spinal dorsal horn, and that the majority of the traced cells are located in the LPGi.

Lateral and midline serotonergic hindbrain neurons display anatomical differences in their spinal cord innervation

Previous anterograde tracing studies have suggested that within the RVM, the innervation of the superficial dorsal horn originates from the lateral hindbrain, whereas the deeper dorsal horn is innervated by the medial hindbrain [26]. The preferential labelling of lateral serotonergic neurons using our intersectional strategy provided us the opportunity to compare the projection patterns of different serotonergic neurons of the hindbrain.

To assess the serotonergic innervation of the spinal cord that originates from the medial RVM we injected AAVs containing Cre-dependent reporters into the nucleus raphe magnus of TPH2::Cre mice (Figure 4A) and were able to label midline serotonergic neurons with eGFP without transduction of the LPGi neurons (Figure 4B). Most eGFP-labelled neurons in

the injection site contained a detectable level of TPH2 (80.5%), indicating this strategy can be used to specifically label midline serotonergic neurons (Figure 4C).

We used tdTomato-expressing vectors to visualize the axon termination pattern of descending serotonergic projections in the spinal cord (Figure 4D and F). For preferential labelling of the LPGi descending neurons, the lumbar spinal cord was injected with AAV2retro vectors containing a Cre-dependent optimized Flippase (AAV2retro.flex.FLPo.BFP), and one week later the hindbrain was injected with AAVs containing flippase-dependent tdTomato (AAV9.FRT.tdTOM). The stronger fluorescence of tdTomato enabled more sensitive labelling of the distal axons of descending projection neurons. The intersectional approach revealed that the densest labelling of axon terminals was present in the superficial laminae of the dorsal horn (Figure 4D, E, and H). Surprisingly, projections retrogradely labelled from the left lumbar spinal cord contained axon collaterals that projected to the contralateral dorsal horn, as well as to spinal segments caudal to the spinal injection site in the lumbar segment (Figure 4E and H). This indicates that these descending neurons have a wide-ranging axon termination pattern that extends over most of the spinal cord.

In contrast, axons from midline serotonergic neurons directly labelled with tdTomato (from injection of AAVs containing a Cre-dependent tdTOM (AAV8.flex.tdTOM) into the NRM (-6, 0, 5.9)) were rarely present in the superficial laminae of the dorsal horn, but they densely innervated the ventral horn and were present in the deep dorsal horn (Figure 4G and I). In both labeling experiments, most of the axon terminals in the spinal cord contained 5-HT, although much of the spinal 5-HT was not colocalized with tdTomato by either labeling approach (Figure 4H and I). Together this indicates that the lateral and midline serotonergic neurons in the RVM project to distinct regions of the spinal cord, in agreement with [26].

Midline and lateral serotonergic hindbrain neurons have similar active and passive membrane properties

Although much is known about the electrophysiological properties of serotonergic hindbrain neurons, to date there has not been a direct comparison of the membrane properties of those located in the NRM or LPGi. To test whether these distinct populations have similar biophysical membrane properties, TPH2::Cre neurons were labelled with tdTomato by hindbrain injection of AAV9.flex.tdTom and targeted for whole-cell recording.

In contrast to their anatomical differences (such as cell soma location and spinal axon termination pattern), TPH2::Cre neurons in the LPGi and NRM had similar active membrane properties and neuronal excitability (Figure 5A and B). In response to depolarizing current steps, these two groups of neurons discharged action potentials that were similar in terms of their thresholds, kinetics, and firing rates (Figure 5A, B, E-G). Cells were labelled with Biocytin during recording, and these groups were distinguished based on the location of biocytin-labelled cell bodies in the hindbrain slice after recording and tissue processing (Figure 5C). Similar to previous reports on the electrophysiological properties of serotonergic RVM neurons, both groups generally had broad action potentials (measured as width at half maximal) and frequently exhibited a slow afterhyperpolarization (9/10 NRM neurons, 5/8 LPGi neurons), which was similar in amplitude between groups (Figure 5A, E, and H) [59]. A summary of these electrophysiological measurements can be found in table 7.

Acute activation of descending serotonergic neurons in the LPGi decreases thermal sensitivity

Descending serotonergic projection neurons can both decrease or increase pain sensitivity, and optogenetic activation of serotonergic neurons of the nucleus raphe magnus produces long-term hypersensitivity to both mechanical and thermal sensitivity [11; 52]. However, intrathecal injection of serotonin can produce acute antinociception [50], and currently little is known of the effect of preferentially activating descending serotonergic neurons in the LPGi.

To clarify whether the acute activation of these serotonergic neurons is pro- or antinociceptive, we used the intersectional strategy to express the excitatory DREADD

hM3D(q) in descending serotonergic neurons of the LPGi (Figure 6A). Although many neurons of the hindbrain were labelled with hM3Dq-mCherry and virtually all mCherry-expressing axon terminals in the lumbar spinal cord contained detectable 5-HT, this only corresponded to a minority of the serotonergic innervation in this area (Figure 6B and C). To exclude the possibility that any observed alteration in sensory behavior was due to impaired motor control or sedation, we first measured the latency to fall from an accelerating rotarod before and after injection of CNO or vehicle. Latency to fall was comparable between animals before and after injection indicating no deficits in sensorimotor coordination or a sedative effect (Repeated measures one-way ANOVA, $F(3, 5) = 0.354$, $P = 0.787$)(Figure 5D)

Despite sparse terminal labelling in the spinal cord, withdrawal latencies to thermal stimuli were increased following CNO injection (Figure 6E). Animals that had received CNO injections exhibited significantly longer withdrawal thresholds to infrared heat stimulation than vehicle injected controls (Repeated measures one-way ANOVA, $F(3, 9) = 10.55$, $P < 0.0001$). Similarly, response latencies to the cold plantar assay were also prolonged following CNO injection (Repeated measures one-way ANOVA, $F(3, 9) = 7.309$, $P = 0.0012$). In contrast, tactile sensitivity to punctate mechanical stimulation with von Frey filaments was unaltered (Repeated measures one-way ANOVA, $F(3, 9) = 1.402$, $P = 0.2666$) (Figure 6E). Together, these data indicate that acute activation of descending serotonergic neurons reduces sensitivity to thermal stimuli, but do not strongly influence mechanical sensitivity.

We also tested the contralateral paw as an internal control for these behavioral experiments. In agreement with the anatomical tracing data (Figure 4E), we saw a significant increase in withdrawal latencies to heat stimulation in the Hargreaves assay (Repeated measures one-way ANOVA, $F(3, 9) = 4.833$, $P = 0.0081$)(Figure 6F). This suggests that the activation of these TPH2::Cre neurons has some influence on the sensitivity of the contralateral paw, presumably via axon collaterals present in the contralateral dorsal horn.

Acute activation of serotonergic neurons in the medial RVM increases mechanical sensitivity

Activation of serotonergic neurons has also been associated with increased sensitivity to tactile and thermal stimuli and is thought to underly certain forms of neuropathic pain [11; 45]. The differences between our findings and those of [11] could be due to either of the mode/strength of serotonergic neuron activation (chemogenetic vs optogenetic) or the anatomical location of the activated neurons (medial hindbrain vs lateral hindbrain). To test this directly, we used the same chemogenetic receptor as our previous experiments to activate midline serotonergic neurons (Figure 7A). Using the same strategy as the anatomical tracing experiment (Figure 4F and G), we injected AAVs containing Cre-dependent hM3Dq.mCherry into the NRM. Similarly, we were able to limit transgene expression to the midline serotonergic neurons without spread to the LPGi (Figure 7B). This resulted in the presence of mCherry-labelled terminals in the deep dorsal horn of the spinal cord, with limited expression in the dense plexus of 5-HT terminals in the superficial spinal laminae (Figure 7C). Again, neither CNO nor vehicle injection impaired sensorimotor coordination or induced sedation, using latency to fall from an accelerating rotarod as a readout measure (Repeated measures one-way ANOVA, $F(3, 6) = 1.791$, $P = 0.185$) (Figure 7D).

In contrast to the activation of serotonergic neurons within the LPGi, the activation of medial RVM neurons had no effect on thermal withdrawal latencies (Repeated measures one-way ANOVA, $F(3, 6) = 0.531$, $P = 0.667$) or responses to cooling (Repeated measures one-way ANOVA, $F(3, 6) = 3.071$, $P = 0.054$) (Figure 7E). However, we observed a significant decrease in the withdrawal thresholds to punctate mechanical stimuli in both the left (Repeated measures one-way ANOVA, $F(3, 6) = 13.84$, $P = 0.787$)(Figure 7E) and right hindpaws (Repeated measures one-way ANOVA, $F(3, 6) = 9.335$ $P = 0.0006$) (Figure 7F). These data indicate that, in contrast to serotonergic neurons of the LPGi, activating medial

serotonergic hindbrain neurons increases mechanical sensitivity without influencing responses to thermal stimuli.

Discussion

Anatomical organization of descending serotonergic innervation of the lumbar spinal cord

The anatomical locations of serotonergic nuclei in the brainstem have been known since the early studies of Dahlstrom and Fuxe [18]. These areas have later been shown to contain spinally-projecting neurons and together provide the spinal cord with serotonin [32]. Similarly, we were also able to label the same regions from the spinal cord with CTb tracing (Figure 2E). However, we found that most of the descending serotonergic neurons transducible by AAV2retro serotype vectors from the mouse spinal cord are located in the LPGi, similar to what has been previously demonstrated [51]. We used this selectivity to devise a strategy to preferentially label midline or lateral serotonergic neurons and demonstrate that, in agreement with anterograde tracing studies, the innervation of the superficial laminae of the dorsal horn mainly originates from the LPGi and not the NRM [26]. The labelling of the midline serotonergic neurons reveals that their axon terminals are present throughout the spinal cord but are notably absent from the superficial laminae. Therefore, it is likely that these pathways influence anatomically distinct neuron populations of the spinal cord, and likely play different functional roles.

The spinal dorsal horn is organized in a laminar structure that is closely linked to its function, such that thermal and nociceptive information is generally received and processed in the superficial laminae, whereas non-nociceptive mechanical and proprioceptive information is processed in deeper spinal laminae [47]. This laminar organization can be seen in terms of gene expression [30], the termination zones of different primary sensory neurons [14; 33], and the restricted laminar location of neuron populations [19]. Therefore, the laminar location of serotonin release will mostly influence different populations of neurons within these regions, which play diverse functional roles [3; 21; 22; 25].

Function of descending LPGi serotonergic neurons in spinal circuits

Acute activation of spinally-projecting serotonergic neurons using excitatory DREADDs was able to reduce sensitivity to thermal tests (Figure 6E and F). In support of this idea, the axons of these projections are densest in the superficial laminae of the spinal cord (Figure 4E and H), where temperature-related information is conveyed by TRPV1- and TRPM8-expressing sensory neurons [13; 14; 20]. The presence of axons from lateral serotonergic neurons within the region that receives, and processes thermal information is consistent with the observation that activating these neurons affects thermal sensitivity. Furthermore, 5-HT can inhibit C fiber-mediated input to the rat superficial dorsal horn and hyperpolarize many types of excitatory neurons in this area, in agreement with a reduction in neuronal activity that would inhibit the relay of temperature-related information [35].

Pronociceptive function of medial serotonergic neurons in spinal circuits

Preclinical models of chronic pain can increase the activity of serotonergic hindbrain neurons, and TPH2 knockdown experiments can transiently reduce spinal 5-HT and hypersensitivity in neuropathic animals [45; 52]. In these neuropathic models, several changes in the physiology of the dorsal horn are widely reported [17; 48; 53]. Together, these pathological changes may alter the way that 5-HT influences the processing of sensory information within the dorsal horn. In agreement, the spinal serotonin receptors engaged by endogenous pain control systems such as diffuse noxious inhibitory controls are altered during the development of chronic pain [4-6]. Additionally, alterations could also occur within the serotonergic projection neurons, such as their activity and neurotransmitter content/concentration [49].

However, there are also data that point to a pro-nociceptive role for 5-HT at the spinal level in naïve animals. For example, it was shown that optogenetic stimulation of the NRM of TPH2-ChR2 animals could induce hypersensitivity that lasted several weeks [11]. In our chemogenetic experiments, the activation of NRM neurons with CNO did produce an

increase in mechanical sensitivity, but unlike Cai *et al* [11] we did not see an alteration in thermal sensitivity or an effect that outlasted the neuron stimulation. These differences could be explained in part by the intensity and location of the stimulation used in experiments. In support of this idea, activation of the same neuron population with optogenetic or chemogenetic tools can produce distinct behaviors, likely due to differences in the strength or pattern of the neuronal activation [44].

Together the results of the chemogenetic experiments indicate that the same transmitter released into different spinal laminae can produce opposing effects on spinal nociception. Potential explanations for these findings include the 5-HTR subtypes that are engaged, the spinal neuron populations that are modulated, or a combination of both. Some 5-HTRs are known to have an excitatory influence when activated, whereas others have an inhibitory effect upon ligand binding [1; 7; 35]. The activation of excitatory neurons and the inhibition of inhibitory neurons in the deep dorsal horn, corresponding to the termination zone of the medial serotonergic neurons, are known increase mechanical sensitivity [21; 22; 39; 40]. Conversely, the activation of inhibitory neurons in the superficial dorsal horn, the region innervated by the lateral serotonergic neurons, and the inhibition of nociceptors through presynaptic inhibition of their central terminals could promote thermal hyposensitivity [31; 35; 57]. Further studies are required to elucidate precisely which spinal 5-HT receptors and neuronal elements are mediating these opposing sensory phenomena.

Limitations of monosynaptic rabies tracing of serotonergic RVM neurons

Monosynaptic rabies tracing has been widely used in recent years to identify presynaptic inputs to genetically defined neuronal populations and has become a frequently used tool for the study of neuronal circuits. Functional studies are limited due to the toxicity of first generation ΔG rabies viruses, although new double deleted variants of the rabies virus that lack both G and L genes have been developed for the long-term studies of monosynaptically traced neurons [15]. However, other limitations of this technique are known, such as the

resistance of some neuronal types to infection by modified rabies viruses [2]. We show that descending TPH2-expressing neurons are not resistant to infection from G-protein deficient rabies viruses, although they are rarely traced monosynaptically from dorsal horn neurons (Figure 1C and F). The lack of transsynaptic labelling from the dorsal horn is possibly due to the synaptic organization of serotonergic axons in the dorsal horn, since serotonin is known to be transmitted via volume transmission [43].

Most serotonergic axons in the rat dorsal horn do not form synaptic contacts [36; 43]. However, some 5-HT-containing axonal boutons do form synapses within the dorsal horn, and these are observed as symmetrical synapses [41]. These synapses contain ionotropic $5HT_3$ receptors, which are the only ligand-gated ion channels of the 5-HT receptors and required for fast serotonergic transmission [7]. In the dorsal horn, these are known to be expressed on the terminals of primary afferent fibres and some lamina I projection neurons [1; 16; 41]. Consistent with the expression of $5\text{-}HT_3$ receptors on the central terminals of primary afferents, monosynaptic rabies tracing from primary afferents does label TPH2-containing hindbrain neurons, suggesting that descending serotonergic neurons can form axo-axonic synapses with the central terminals of primary afferents [61]. In the present study, the number of primary afferent neurons transduced from intraspinal injection of helper virus is likely small, since the AAV8 serotype and the inclusion of the hSyn promoter were used to reduce the transduction of sensory neurons [27]. This is consistent with the low number of mCherry-expressing cells found in the DRG taken from these animals. Since projection neurons are approximately 5% of all lamina I neurons [12], the monosynaptic tracing from these neurons may not be detected in our experiments. The population of inhibitory neurons that expresses the $5\text{-}HT_3$ receptor may also be very small or not express these receptors in synaptic structures. In support of this, most $5\text{-}HT_3$ receptors are expressed on axon terminals, which may be difficult to trace transsynaptically with modified rabies viruses. This may explain why so few serotonergic hindbrain neurons were traced transsynaptically from the spinal dorsal horn [23; 34].

Preferential transduction of LPGi serotonergic neurons with AAV2retro serotype vectors

The AAV2retro serotype has been developed for the retrograde delivery of genetic material to projection neurons via their axon terminals in a target region [46]. Many projection neurons are found to display some resistance to transduction with these tools, for example dopaminergic neurons that project from the substantia nigra to the striatum and descending noradrenergic neurons of the locus coeruleus to the spinal cord [24; 46]. Like others, we also find that NRM serotonergic neurons are largely resistant to AAV2retro-mediated transduction [51]. Surprisingly, we observed that the located serotonergic neurons of the lateral hindbrain do not display such resistance (Figure 2G and H). This would suggest that these neurons are different in some property that allows the AAV2retro to enter their terminals or enhances the retrograde transport of the viral payload. The increased retrograde labelling efficiency of AAV2retro is not fully understood, although enhanced entry into axon terminals by increased spread of the vector in the injection site, entry into neurons via novel cell surface receptor interactions, and vesicular trafficking have been suggested [46]. AAV2retro-resistant neurons commonly use monoamines as neurotransmitters, suggesting that they likely share common features protecting them from transduction by these vectors.

Primarily, this data establishes descending serotonergic neurons originating in the LPGi as antinociceptive during acute activation. These neurons project their axons to the superficial laminae of the dorsal horn and can be targeted using AAV2retro vectors. In contrast, the medial serotonergic neurons are resistant to AAV2retro-mediated transduction, produce mechanical hypersensitivity upon acute activation, and project their axons to the deeper dorsal horn. Secondly, we highlight some of the limitations and challenges associated with AAV2retro-mediated and rabies virus-based monosynaptic tracing from the spinal dorsal horn. These limitations are likely to have broader implications for monosynaptic rabies-based circuit tracing and the targeting of other projections that use biogenic amines, and possibly other transmitter systems.

Figure 1: labelling of spinally-projecting serotonergic neurons with direct rabies infection and monosynaptic rabies tracing. A. Injection strategy for the direct labelling of spinally-projecting hindbrain neurons with a SAD pseudotyped and G-protein deficient rabies virus. B. Example of a cell body of a labelled hindbrain neuron that is immunoreactive for TPH2 (scale bar = 50 μm). C. Quantification of the GFP-labelled hindbrain neurons that express detectable levels of TPH2. Note that 7 days after rabies virus injection there are fewer labelled neurons that express TPH2. N = 3 animals. D. Injection strategy for the monosynaptic tracing of neurons from spinal dorsal horn neurons. Hoxb8-Cre is transiently expressed in all lumbar dorsal horn neurons and is crossed with ROSA26^{TVA} to induce TVA expression in all spinal neurons. E. Example of an infected cell monosynaptically traced RVM neuron from the spinal dorsal horn (scale bar = 50 μm) F. Quantification of GFP-labelled neurons in the hindbrain that express detectable TPH2. Data from C. "5 days post injection" is included to allow comparison between directly labelled and monosynaptically traced neurons. N = 4 animals for monosynaptic tracing experiment.

Figure 2: Retrograde labelling of spinally-projecting serotonergic neurons with AAV2retro vectors and Cholera toxin b subunit. A. Injection scheme for retrograde labelling of spinally-projecting neurons with AAV2retro.eGFP. B Image of the ventral hindbrain containing eGFP-labelled neurons (scale bar = 200 μm). Inset shows enlargement of the LPGi to reveal eGFP neurons that also express TPH2. C. Quantification of cell location for eGFP-labelled neurons that express TPH2. Each datapoint is a count per animal (5-7 sections per animal) D. injection scheme for CTb tracing from the lumbar dorsal horn and an example of the injection site in the lumbar spinal cord (scale bar = 200 μm). E. Example of a hindbrain section from the injection site shown in D (scale bars = 200 μm). The inset shows that many CTb labelled neurons that express TPH2 are found in the nucleus raphe magnus F. Injection scheme for retrograde tracing from the spinal dorsal horn with AAV2retro.GFP and CTb. G. Representative image of the ventral hindbrain containing CTb-labelled and AAV2retro-transduced projection neurons (scale bar = 200 μm). H. Quantification of

coexpression of CTb and eGFP in all retrogradely-labelled RVM neurons, and quantification of coexpression of CTb and eGFP in retrogradely-traced neurons that contain TPH2. This quantification is performed for all retrogradely-labelled TPH2-containing neurons, as well as for the retrogradely-labelled neurons in different hindbrain regions.

Figure 3: Labelling of spinally-projecting neurons in the TPH2::Cre mouse with AAV2retro vectors. A. Injection scheme for labelling spinally-projecting TPH2::Cre neurons. B. An example of a hindbrain section containing neurons labelled with eGFP (scale bar = 200 μm). Inset is an enlargement of the area indicated in the dashed box, with many eGFP labelled cells found to express detectable TPH2 that are indicated with arrows. C. Image of an ipsilateral DRG from a TPH2::Cre that received a spinal injection of AAV2retro.flex.eGFP, showing many eGFP-expressing neurons (scale bar = 100 μm). D. Quantification of the location of eGFP labelled cells in the hindbrain. E. Quantification of the hindbrain neurons labelled with eGFP that also contain TPH2. For D. and E. each datapoint is a count per animal (n = 3 animals). F. Injection scheme for the intersectional labelling of spinally-projecting TPH2::Cre neurons. Brain injection coordinates (-6, +/-0.5, 5.9) from bregma, for the labelling of spinally-projecting TPH2::Cre neurons in the LPGi, according to the mouse brain atlas. Target injection sites are indicated in red crosshairs. G. Example of a hindbrain section from a TPH2::Cre mouse that received the injections illustrated in F (scale bar = 500 μm). Inset is an enlargement of the boxed area and highlights neurons that were captured with the brain injection and express eGFP (arrowheads) as well as neurons that were directly labelled from the spinal cord injection (mCherry+) that were not transduced from the hindbrain injection (arrows). Scale bar = 200 μm) H. Quantification of the mCherry-expressing cells that are labelled with eGFP, which indicated that they were captured with the hindbrain injection. The percentages of mCherry-only and eGFP-only cells are also quantified for each hindbrain area that contains serotonergic neurons, and areas that could not be assigned as either NRM or LPGi were classified as “other” (n = 4 animals)

Figure 4: Spinal cord regions innervated by serotonergic hindbrain neurons. A. Injection scheme for labelling medially located serotonergic neurons of the hindbrain with AAVs. Stereotaxic injection coordinates for the hindbrain injection of AAVs to label midline neurons without transducting LPGi serotonergic neurons (-6, 0, 5.9). B. Representative brain injection site from the hindbrain of a TPH2::Cre mouse that received a single 300nl injection of AAV8.hSyn.flex.eGFP). Scale bar = 500 μm. Higher magnification of the injection site in B, scale bar = 100 μm. C. Quantification of the proportion of eGFP-labelled neurons in the injection site that were immunoreactive for TPH2. D. Intersectional strategy to preferentially label the spinal axon terminals of descending serotonergic neurons that originate in the LPGi. E. Representative images of the hindbrain injection site and spinal cord axon termination pattern of a TPH2::Cre animal that received the injections depicted in D (scale bars = 500 μm and 100 μm for hindbrain and spinal cord sections respectively). F. Injection scheme for labelling medially located serotonergic neurons with tdTOM. G. Representative images of the hindbrain injection site and spinal cord axon termination pattern of a TPH2::Cre animal that received a single 300nl injection of AAV8.hSyn.flex.tdTOM depicted in F (scale bars = 500 μm and 100 μm for hindbrain and spinal cord sections respectively). H. Higher magnification images of the cervical and lumbar dorsal horns of a TPH2::Cre animal that received the injections depicted in D (scale bar = 100 μm). I. Representative images from cervical and lumbar spinal cord segments of animals that received an injection with AAV8.hSyn.flex.tdTOM into the NRM (scale bar = 100 μm).

Figure 5: Electrophysiological characterization of serotonergic neurons of the NRM and the LPGi. A. Current step protocol (red) and resulting AP firing (black) from representative serotonergic NRM and LPGi neurons recorded in current clamp. B. Current/frequency plot for the AP firing frequency of NRM and LPGi neurons resulting from increasing 1s depolarizing current injections. C. Representative images of biocytin filled neurons within the NRM and LPGi of hindbrain slices revealed following recording (scale bar

= 200 μm). D – H comparison of active and passive membrane properties between NRM and LPGi serotonergic neurons. D – G. n = 10 NRM n = 8 LPGi. H. n = 9 NRM n = 5 LPGi

Figure 6: Chemogenetic activation of descending serotonergic LPGi neurons. A. Injection scheme for expressing the excitatory DREADD hM3Dq in spinally-projecting TPH2::Cre neurons. Brain injection coordinates according to the mouse brain atlas (-6, +/- 0.5, 5.9 from bregma). B. Example of the injection site from the hindbrain of a mouse that received a spinal dorsal horn injection of AAV2retro.flex.FLPo.BFP followed by a bilateral hindbrain injection of AAV1.FRT.hM3Dq.mCherry one week later (scale bar = 200 μm). C. Example of the ipsilateral spinal dorsal horn form an animal that had received the injections indicated in A . Note that most 5-HT-containing terminals are not labelled, but the majority of labelled terminals contain a detectable level of 5-HT (scale bar = 200 μm). D. Rotarod test for sensorimotor coordination/sedation; repeated measures one-way ANOVA, ($F(3, 5) = 0.354$, $P = 0.787$). E. Sensory tests of the ipsilateral hindpaw: Hargreaves plantar assay; repeated measures one-way ANOVA, ($F(3, 9) = 10.55$, $P < 0.0001$). Cold plantar assay; repeated measures one-way ANOVA, ($F(3, 9) = 7.309$, $P = 0.0012$). von Frey test; repeated measures one-way ANOVA, ($F(3, 9) = 1.402$, $P = 0.2666$). F. Sensory tests of the contralateral hindpaw: Hargreaves plantar assay; repeated measures one-way ANOVA, ($F(3, 9) = 4.833$, $P = 0.0081$).

Figure 7: Chemogenetic activation of medial serotonergic hindbrain neurons. A. Injection scheme for chemogenetic activation of medial serotonergic hindbrain neurons. Stereotaxic coordinates used for activating midline serotonergic neurons of TPH2::Cre animals with hM3D(q)-containing AAVs (-6, 0, 5.9). C. Example of an injection site from an experiment to activate midline serotonergic neurons with hM3D(q). D. Lumbar spinal cord from the injection site shown in C. showing mCherry-expressing terminals located ventral to the dense 5-HT innervation of the superficial dorsal horn. F and G. Sensory assays of animals following CNO or Vehicle injections in the left and right hindpaw. Repeated one-way

ANOVA, followed by Bonferonni post-hoc tests for von Frey left ($F(3, 6) = 13.84$, $P < 0.0001$) and right hindpaws ($F(3, 6) = 9.335$, $P = 0.0006$) show significant decreases between Vehicle and CNO injections.

References

[1] Abe K, Kato G, Katafuchi T, Tamae A, Furue H, Yoshimura M. Responses to 5-HT in morphologically identified neurons in the rat substantia gelatinosa in vitro. Neuroscience 2009;159(1):316-324.

[2] Albisetti GW, Ghanem A, Foster E, Conzelmann KK, Zeilhofer HU, Wildner H. Identification of Two Classes of Somatosensory Neurons That Display Resistance to Retrograde Infection by Rabies Virus. J Neurosci 2017;37(43):10358-10371.

[3] Albisetti GW, Pagani M, Platonova E, Hösli L, Johannssen HC, Fritschy JM, Wildner H, Zeilhofer HU. Dorsal Horn Gastrin-Releasing Peptide Expressing Neurons Transmit Spinal Itch But Not Pain Signals. J Neurosci 2019;39(12):2238-2250.

[4] Bannister K, Dickenson AH. What do monoamines do in pain modulation? Curr Opin Support Palliat Care 2016;10(2):143-148.

[5] Bannister K, Lockwood S, Goncalves L, Patel R, Dickenson AH. An investigation into the inhibitory function of serotonin in diffuse noxious inhibitory controls in the neuropathic rat. Eur J Pain 2017;21(4):750-760.

[6] Bannister K, Patel R, Goncalves L, Townson L, Dickenson AH. Diffuse noxious inhibitory controls and nerve injury: restoring an imbalance between descending monoamine inhibitions and facilitations. Pain 2015;156(9):1803-1811.

[7] Bardoni R. Serotonergic Modulation of Nociceptive Circuits in Spinal Cord Dorsal Horn. Curr Neuropharmacol 2019;17(12):1133-1145.

[8] Basbaum AI, Clanton CH, Fields HL. Opiate and stimulus-produced analgesia: functional anatomy of a medullospinal pathway. Proc Natl Acad Sci U S A 1976;73(12):4685-4688.

[9] Basbaum AI, Fields HL. Endogenous pain control systems: brainstem spinal pathways and endorphin circuitry. Annu Rev Neurosci 1984;7:309-338.

[10] Basbaum AI, Marley NJ, O'Keefe J, Clanton CH. Reversal of morphine and stimulus-produced analgesia by subtotal spinal cord lesions. Pain 1977;3(1):43-56.

[11] Cai YQ, Wang W, Hou YY, Pan ZZ. Optogenetic activation of brainstem serotonergic neurons induces persistent pain sensitization. Mol Pain 2014;10:70.

[12] Cameron D, Polgár E, Gutierrez-Mecinas M, Gomez-Lima M, Watanabe M, Todd AJ. The organisation of spinoparabrachial neurons in the mouse. Pain 2015;156(10):2061-2071.

[13] Cavanaugh DJ, Chesler AT, Jackson AC, Sigal YM, Yamanaka H, Grant R, O'Donnell D, Nicoll RA, Shah NM, Julius D, Basbaum AI. Trpv1 reporter mice reveal highly restricted brain distribution and functional expression in arteriolar smooth muscle cells. J Neurosci 2011;31(13):5067-5077.

[14] Cavanaugh DJ, Lee H, Lo L, Shields SD, Zylka MJ, Basbaum AI, Anderson DJ. Distinct subsets of unmyelinated primary sensory fibers mediate behavioral responses to noxious thermal and mechanical stimuli. Proc Natl Acad Sci U S A 2009;106(22):9075-9080.

[15] Chatterjee S, Sullivan HA, MacLennan BJ, Xu R, Hou Y, Lavin TK, Lea NE, Michalski JE, Babcock KR, Dietrich S, Matthews GA, Beyeler A, Calhoon GG, Glober G, Whitesell JD, Yao S, Cetin A, Harris JA, Zeng H, Tye KM, Reid RC, Wickersham IR. Nontoxic, double-deletion-mutant rabies viral vectors for retrograde targeting of projection neurons. Nat Neurosci 2018;21(4):638-646.

[16] Conte D, Legg ED, McCourt AC, Silajdzic E, Nagy GG, Maxwell DJ. Transmitter content, origins and connections of axons in the spinal cord that possess the serotonin (5-hydroxytryptamine) 3 receptor. Neuroscience 2005;134(1):165-173.

[17] Coull JA, Boudreau D, Bachand K, Prescott SA, Nault F, Sík A, De Koninck P, De Koninck Y. Trans-synaptic shift in anion gradient in spinal lamina I neurons as a mechanism of neuropathic pain. Nature 2003;424(6951):938-942.

[18] Dahlstrom A, Fuxe K. Localization of monoamines in the lower brain stem. Experientia 1964;20(7):398-399.

[19] Das Gupta RR, Scheurer L, Pelczar P, Wildner H, Zeilhofer HU. Neuron-specific spinal cord translatomes reveal a neuropeptide code for mouse dorsal horn excitatory neurons. Sci Rep 2021;11(1):5232.
[20] Dhaka A, Earley TJ, Watson J, Patapoutian A. Visualizing cold spots: TRPM8-expressing sensory neurons and their projections. J Neurosci 2008;28(3):566-575.
[21] Duan B, Cheng L, Bourane S, Britz O, Padilla C, Garcia-Campmany L, Krashes M, Knowlton W, Velasquez T, Ren X, Ross S, Lowell BB, Wang Y, Goulding M, Ma Q. Identification of spinal circuits transmitting and gating mechanical pain. Cell 2014;159(6):1417-1432.
[22] Foster E, Wildner H, Tudeau L, Haueter S, Ralvenius WT, Jegen M, Johannssen H, Hösli L, Haenraets K, Ghanem A, Conzelmann KK, Bösl M, Zeilhofer HU. Targeted ablation, silencing, and activation establish glycinergic dorsal horn neurons as key components of a spinal gate for pain and itch. Neuron 2015;85(6):1289-1304.
[23] Francois A, Low SA, Sypek EI, Christensen AJ, Sotoudeh C, Beier KT, Ramakrishnan C, Ritola KD, Sharif-Naeini R, Deisseroth K, Delp SL, Malenka RC, Luo L, Hantman AW, Scherrer G. A Brainstem-Spinal Cord Inhibitory Circuit for Mechanical Pain Modulation by GABA and Enkephalins. Neuron 2017;93(4):822-839.e826.
[24] Ganley RP, Werder K, Wildner H, Zeilhofer HU. Spinally projecting noradrenergic neurons of the locus coeruleus display resistance to AAV2retro-mediated transduction. Mol Pain 2021;17:17448069211037887.
[25] Gatto G, Bourane S, Ren X, Di Costanzo S, Fenton PK, Halder P, Seal RP, Goulding MD. A Functional Topographic Map for Spinal Sensorimotor Reflexes. Neuron 2020.
[26] Gautier A, Geny D, Bourgoin S, Bernard JF, Hamon M. Differential innervation of superficial versus deep laminae of the dorsal horn by bulbo-spinal serotonergic pathways in the rat. IBRO Rep 2017;2:72-80.
[27] Haenraets K, Albisetti GW, Foster E, Wildner H. Adeno-associated Virus-mediated Transgene Expression in Genetically Defined Neurons of the Spinal Cord. J Vis Exp 2018(135).
[28] Hirschberg S, Li Y, Randall A, Kremer EJ, Pickering AE. Functional dichotomy in spinal- vs prefrontal-projecting locus coeruleus modules splits descending noradrenergic analgesia from ascending aversion and anxiety in rats. Elife 2017;6.
[29] Huang J, Polgár E, Solinski HJ, Mishra SK, Tseng PY, Iwagaki N, Boyle KA, Dickie AC, Kriegbaum MC, Wildner H, Zeilhofer HU, Watanabe M, Riddell JS, Todd AJ, Hoon MA. Circuit dissection of the role of somatostatin in itch and pain. Nat Neurosci 2018;21(5):707-716.
[30] Häring M, Zeisel A, Hochgerner H, Rinwa P, Jakobsson JET, Lönnerberg P, La Manno G, Sharma N, Borgius L, Kiehn O, Lagerström MC, Linnarsson S, Ernfors P. Neuronal atlas of the dorsal horn defines its architecture and links sensory input to transcriptional cell types. Nat Neurosci 2018;21(6):869-880.
[31] Jeong HJ, Mitchell VA, Vaughan CW. Role of 5-HT(1) receptor subtypes in the modulation of pain and synaptic transmission in rat spinal superficial dorsal horn. Br J Pharmacol 2012;165(6):1956-1965.
[32] Kwiat GC, Basbaum AI. The origin of brainstem noradrenergic and serotonergic projections to the spinal cord dorsal horn in the rat. Somatosens Mot Res 1992;9(2):157-173.
[33] Li L, Rutlin M, Abraira VE, Cassidy C, Kus L, Gong S, Jankowski MP, Luo W, Heintz N, Koerber HR, Woodbury CJ, Ginty DD. The functional organization of cutaneous low-threshold mechanosensory neurons. Cell 2011;147(7):1615-1627.
[34] Liu MZ, Chen XJ, Liang TY, Li Q, Wang M, Zhang XY, Li YZ, Sun Q, Sun YG. Synaptic control of spinal GRPR(+) neurons by local and long-range inhibitory inputs. Proc Natl Acad Sci U S A 2019.
[35] Lu Y, Perl ER. Selective action of noradrenaline and serotonin on neurones of the spinal superficial dorsal horn in the rat. J Physiol 2007;582(Pt 1):127-136.
[36] Maxwell DJ, Leranth C, Verhofstad AA. Fine structure of serotonin-containing axons in the marginal zone of the rat spinal cord. Brain Res 1983;266(2):253-259.
[37] Millan MJ. Descending control of pain. Prog Neurobiol 2002;66(6):355-474.

[38] Pedersen NP, Vaughan CW, Christie MJ. Opioid receptor modulation of GABAergic and serotonergic spinally projecting neurons of the rostral ventromedial medulla in mice. J Neurophysiol 2011;106(2):731-740.
[39] Peirs C, Williams SG, Zhao X, Arokiaraj CM, Ferreira DW, Noh MC, Smith KM, Halder P, Corrigan KA, Gedeon JY, Lee SJ, Gatto G, Chi D, Ross SE, Goulding M, Seal RP. Mechanical Allodynia Circuitry in the Dorsal Horn Is Defined by the Nature of the Injury. Neuron 2020.
[40] Peirs C, Williams SP, Zhao X, Walsh CE, Gedeon JY, Cagle NE, Goldring AC, Hioki H, Liu Z, Marell PS, Seal RP. Dorsal Horn Circuits for Persistent Mechanical Pain. Neuron 2015;87(4):797-812.
[41] Polgar E, Puskar Z, Watt C, Matesz C, Todd AJ. Selective innervation of lamina I projection neurones that possess the neurokinin 1 receptor by serotonin-containing axons in the rat spinal cord. Neuroscience 2002;109(4):799-809.
[42] Porreca F, Burgess SE, Gardell LR, Vanderah TW, Malan TP, Jr., Ossipov MH, Lappi DA, Lai J. Inhibition of neuropathic pain by selective ablation of brainstem medullary cells expressing the mu-opioid receptor. J Neurosci 2001;21(14):5281-5288.
[43] Ridet JL, Rajaofetra N, Teilhac JR, Geffard M, Privat A. Evidence for nonsynaptic serotonergic and noradrenergic innervation of the rat dorsal horn and possible involvement of neuron-glia interactions. Neuroscience 1993;52(1):143-157.
[44] Sharif B, Ase AR, Ribeiro-da-Silva A, Séguéla P. Differential Coding of Itch and Pain by a Subpopulation of Primary Afferent Neurons. Neuron 2020;106(6):940-951.e944.
[45] Suzuki R, Morcuende S, Webber M, Hunt SP, Dickenson AH. Superficial NK1-expressing neurons control spinal excitability through activation of descending pathways. Nat Neurosci 2002;5(12):1319-1326.
[46] Tervo DG, Hwang BY, Viswanathan S, Gaj T, Lavzin M, Ritola KD, Lindo S, Michael S, Kuleshova E, Ojala D, Huang CC, Gerfen CR, Schiller J, Dudman JT, Hantman AW, Looger LL, Schaffer DV, Karpova AY. A Designer AAV Variant Permits Efficient Retrograde Access to Projection Neurons. Neuron 2016;92(2):372-382.
[47] Todd AJ. Neuronal circuitry for pain processing in the dorsal horn. Nat Rev Neurosci 2010;11(12):823-836.
[48] Todd AJ. Plasticity of inhibition in the spinal cord. Handb Exp Pharmacol 2015;227:171-190.
[49] Tudeau L, Acuña MA, Albisetti GW, Neumann E, Ralvenius WT, Scheurer L, Poe M, Cook JM, Johannssen HC, Zeilhofer HU. Mice lacking spinal α2GABA(A) receptors: Altered GABAergic neurotransmission, diminished GABAergic antihyperalgesia, and potential compensatory mechanisms preventing a hyperalgesic phenotype. Brain Res 2020;1741:146889.
[50] Wang JK. Antinociceptive effect of intrathecally administered serotonin. Anesthesiology 1977;47(3):269-271.
[51] Wang Z, Maunze B, Wang Y, Tsoulfas P, Blackmore MG. Global Connectivity and Function of Descending Spinal Input Revealed by 3D Microscopy and Retrograde Transduction. J Neurosci 2018;38(49):10566-10581.
[52] Wei F, Dubner R, Zou S, Ren K, Bai G, Wei D, Guo W. Molecular depletion of descending serotonin unmasks its novel facilitatory role in the development of persistent pain. J Neurosci 2010;30(25):8624-8636.
[53] West SJ, Bannister K, Dickenson AH, Bennett DL. Circuitry and plasticity of the dorsal horn--toward a better understanding of neuropathic pain. Neuroscience 2015;300:254-275.
[54] Wickersham IR, Finke S, Conzelmann KK, Callaway EM. Retrograde neuronal tracing with a deletion-mutant rabies virus. Nat Methods 2007;4(1):47-49.
[55] Wickersham IR, Lyon DC, Barnard RJ, Mori T, Finke S, Conzelmann KK, Young JA, Callaway EM. Monosynaptic restriction of transsynaptic tracing from single, genetically targeted neurons. Neuron 2007;53(5):639-647.
[56] Witschi R, Johansson T, Morscher G, Scheurer L, Deschamps J, Zeilhofer HU. Hoxb8-Cre mice: A tool for brain-sparing conditional gene deletion. Genesis 2010;48(10):596-602.
[57] Xie DJ, Uta D, Feng PY, Wakita M, Shin MC, Furue H, Yoshimura M. Identification of 5-HT receptor subtypes enhancing inhibitory transmission in the rat spinal dorsal horn in vitro. Mol Pain 2012;8:58.

[58] Yesilyurt O, Seyrek M, Tasdemir S, Kahraman S, Deveci MS, Karakus E, Halici Z, Dogrul A. The critical role of spinal 5-HT7 receptors in opioid and non-opioid type stress-induced analgesia. Eur J Pharmacol 2015;762:402-410.
[59] Zhang L, Sykes KT, Buhler AV, Hammond DL. Electrophysiological heterogeneity of spinally projecting serotonergic and nonserotonergic neurons in the rostral ventromedial medulla. J Neurophysiol 2006;95(3):1853-1863.
[60] Zhang W, Gardell S, Zhang D, Xie JY, Agnes RS, Badghisi H, Hruby VJ, Rance N, Ossipov MH, Vanderah TW, Porreca F, Lai J. Neuropathic pain is maintained by brainstem neurons co-expressing opioid and cholecystokinin receptors. Brain 2009;132(Pt 3):778-787.
[61] Zhang Y, Zhao S, Rodriguez E, Takatoh J, Han BX, Zhou X, Wang F. Identifying local and descending inputs for primary sensory neurons. J Clin Invest 2015;125(10):3782-3794.

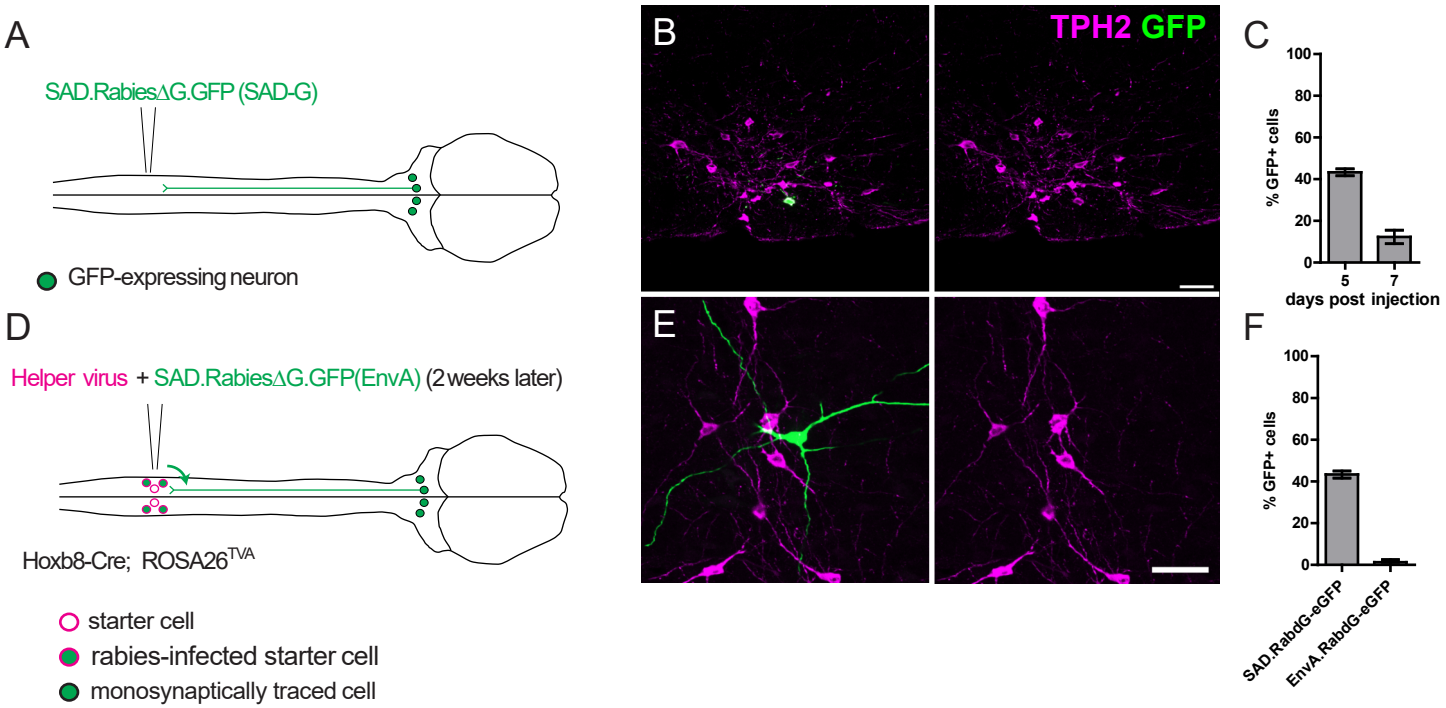
A
SAD.RabiesΔG.GFP (SAD-G)
GFP-expressing neuron
B
TPH2 GFP
C
% GFP+ cells
100
80
60
40
20
0
5
7
days post injection
D
Helper virus + SAD.RabiesΔG.GFP(EnvA) (2 weeks later)
Hoxb8-Cre; ROSA26TVA
starter cell
rabies-infected starter cell
monosynaptically traced cell
E
F
% GFP+ cells
100
80
60
40
20
0
SAD.RabdG-eGFP
EnvA.RabdG-eGFP

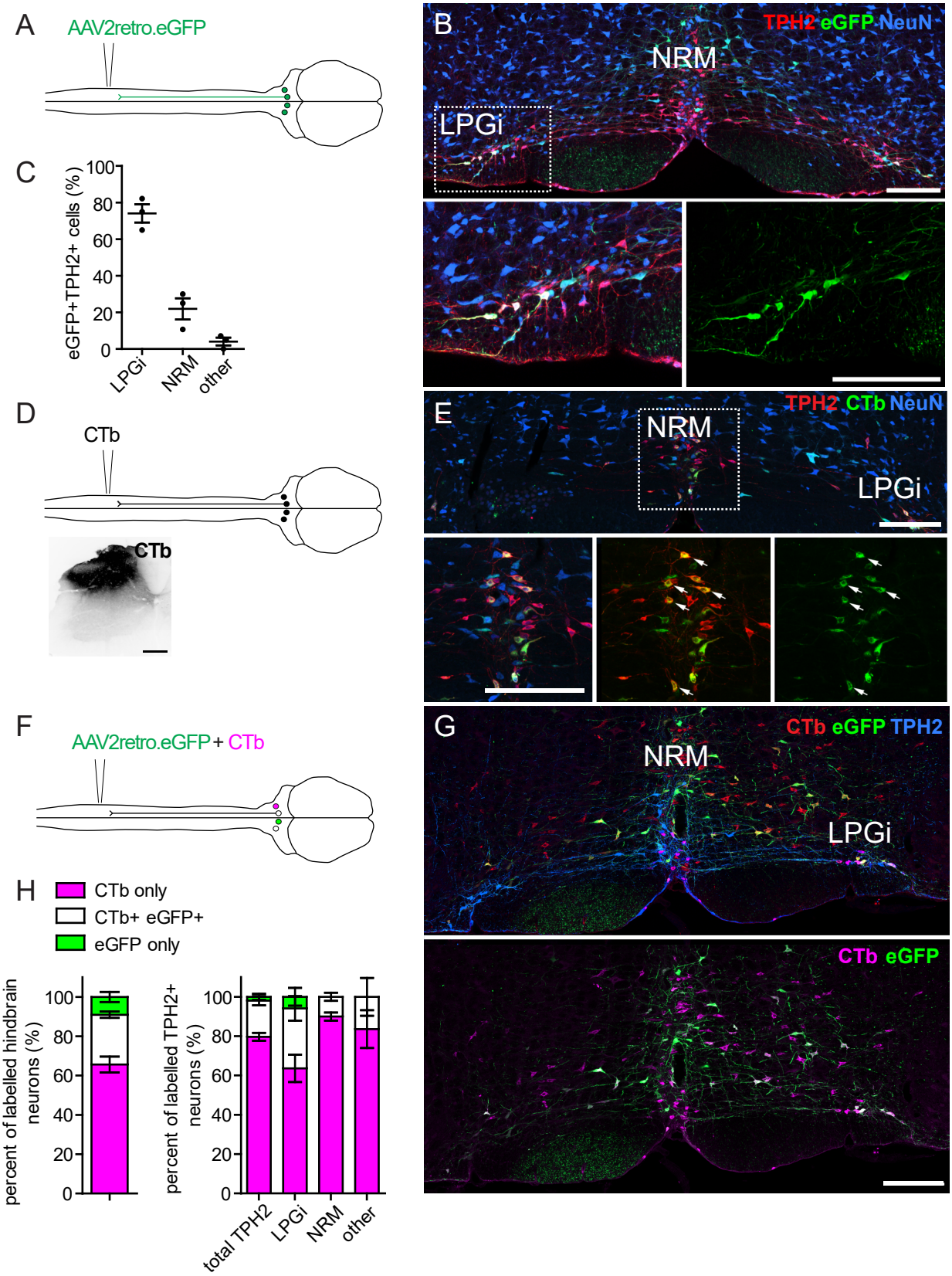
A
AAV2retro.eGFP
B
TPH2 eGFP NeuN
NRM
LPGi
C
eGFP+TPH2+ cells (%)
100
80
60
40
20
0
LPGi
NRM
other
D
CTb
CTb
E
TPH2 CTb NeuN
NRM
LPGi
F
AAV2retro.eGFP + CTb
G
CTb eGFP TPH2
NRM
LPGi
CTb eGFP
H
CTb only
CTb+ eGFP+
eGFP only
percent of labelled hindbrain neurons (%)
percent of labelled TPH2+ neurons (%)
total TPH2
LPGi
NRM
other

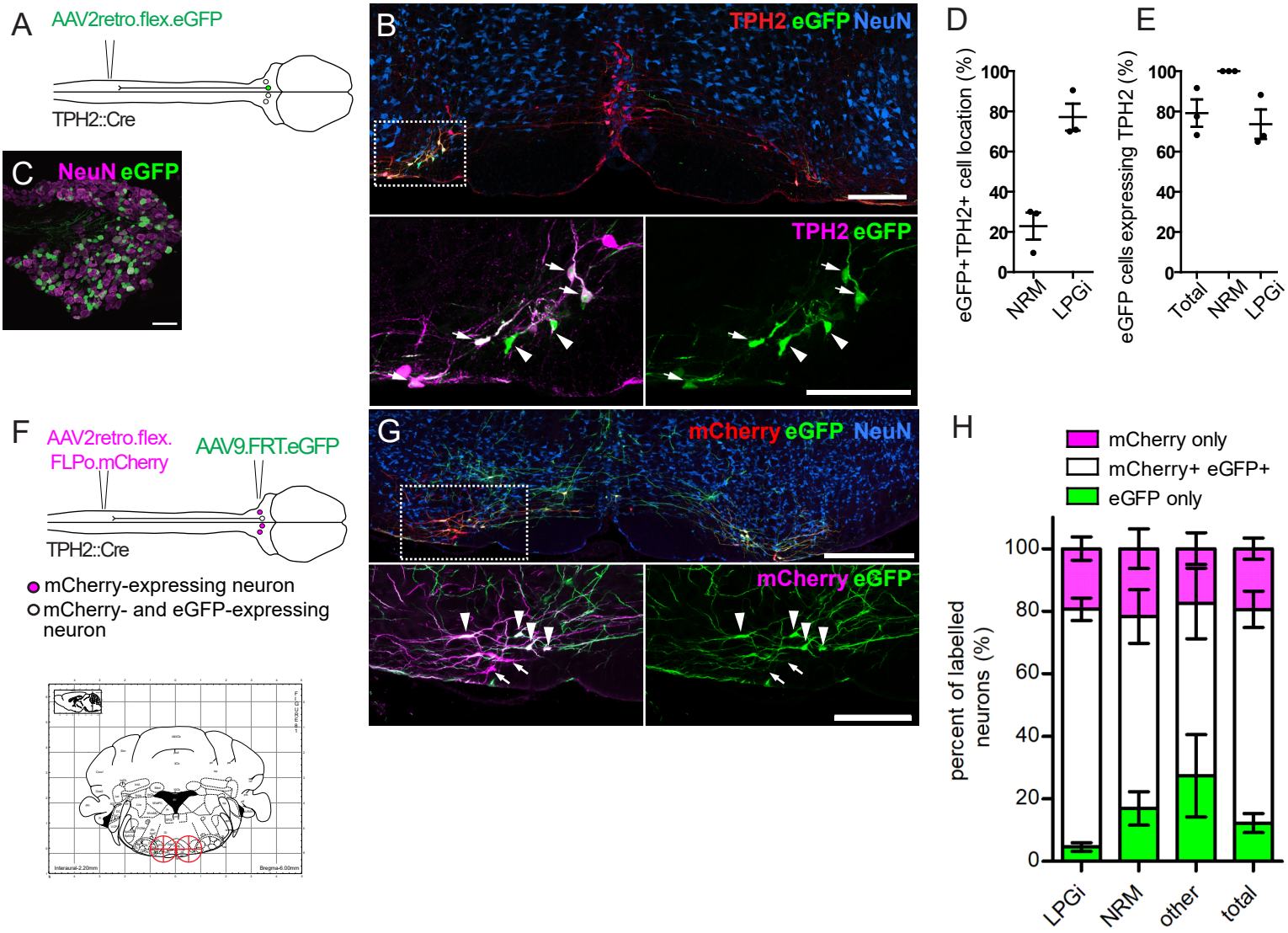
A
AAV2retro.flex.eGFP
TPH2::Cre
B
TPH2 eGFP NeuN
TPH2 eGFP
C
NeuN eGFP
D
eGFP+TPH2+ cell location (%)
100
80
60
40
20
0
NRM
LPGi
E
eGFP cells expressing TPH2 (%)
Total
NRM
LPGi
F
AAV2retro.flex.
FLPo.mCherry
AAV9.FRT.eGFP
TPH2::Cre
mCherry-expressing neuron
mCherry- and eGFP-expressing neuron
G
mCherry eGFP NeuN
mCherry eGFP
H
mCherry only
mCherry+ eGFP+
eGFP only
percent of labelled neurons (%)
LPGi
NRM
other
total

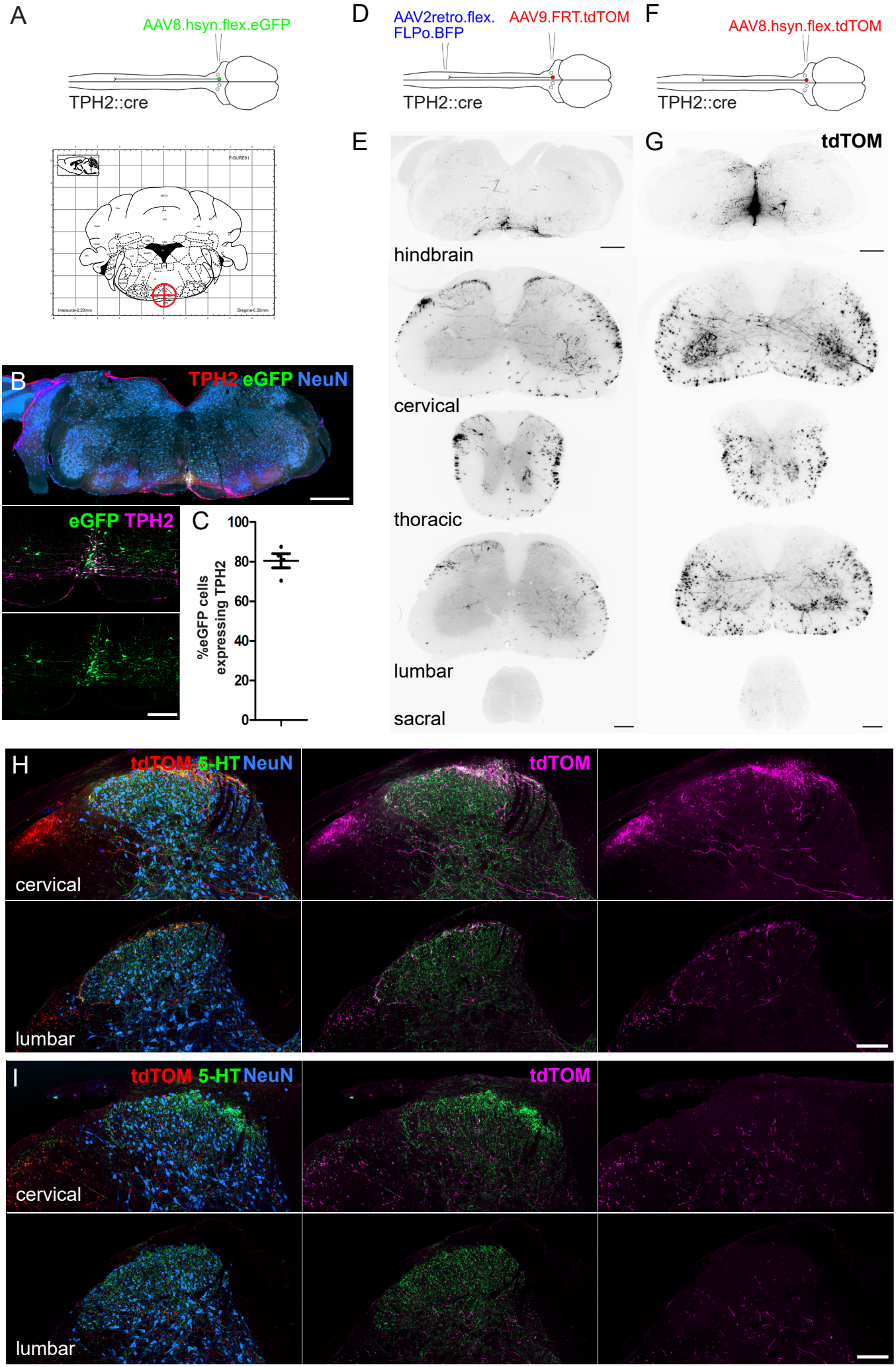
A
AAV8.hsyn.flex.eGFP
TPH2::cre
D
AAV2retro.flex.
FLPo.BFP
AAV9.FRT.tdTOM
TPH2::cre
F
AAV8.hsyn.flex.tdTOM
TPH2::cre
B
TPH2 eGFP NeuN
eGFP TPH2
C
%eGFP cells
expressing TPH2
100
80
60
40
20
0
E
hindbrain
cervical
thoracic
lumbar
sacral
G
tdTOM
H
tdTOM 5-HT NeuN
tdTOM
cervical
lumbar
I
tdTOM 5-HT NeuN
tdTOM
cervical
lumbar

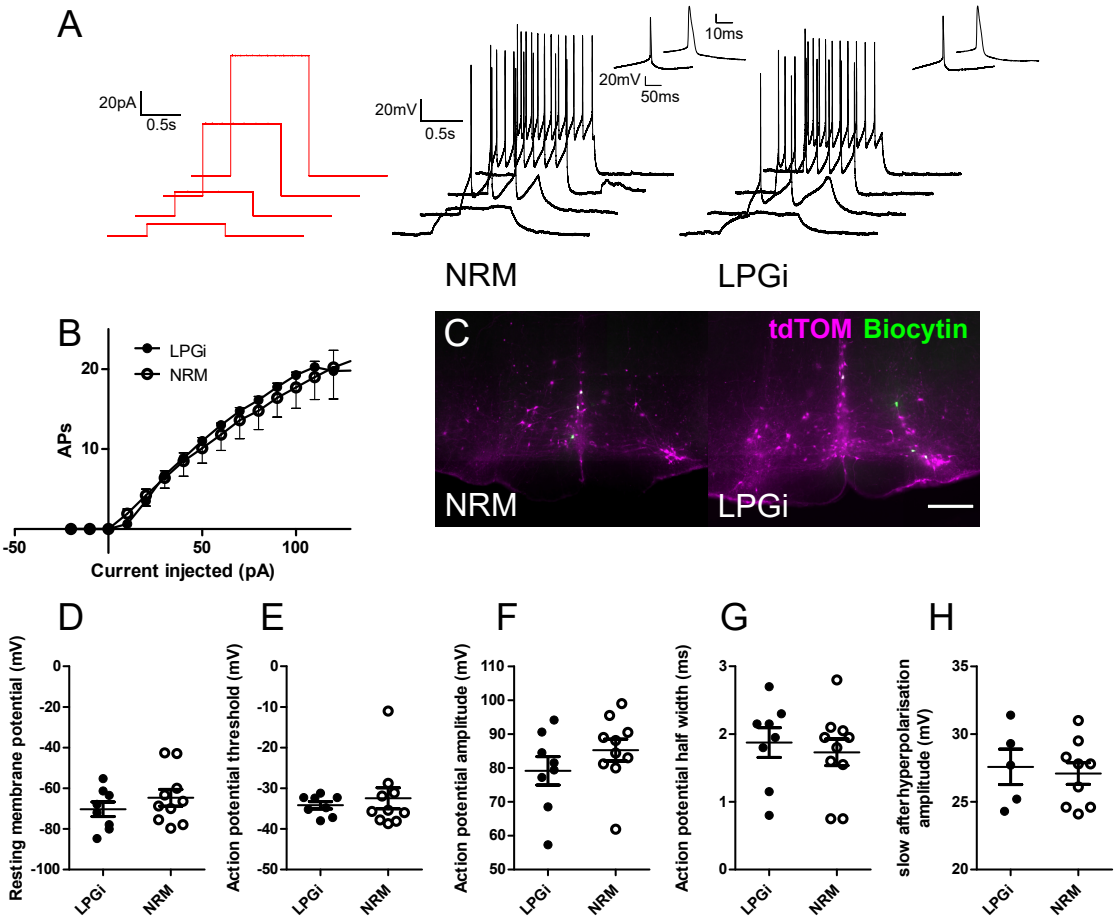
A
20pA
0.5s
20mV
0.5s
10ms
20mV
50ms
NRM
LPGi
B
LPGi
NRM
APs
Current injected (pA)
C
tdTOM Biocytin
NRM
LPGi
D
Resting membrane potential (mV)
E
Action potential threshold (mV)
F
Action potential amplitude (mV)
G
Action potential half width (ms)
H
slow afterhyperpolarisation amplitude (mV)
LPGi
NRM

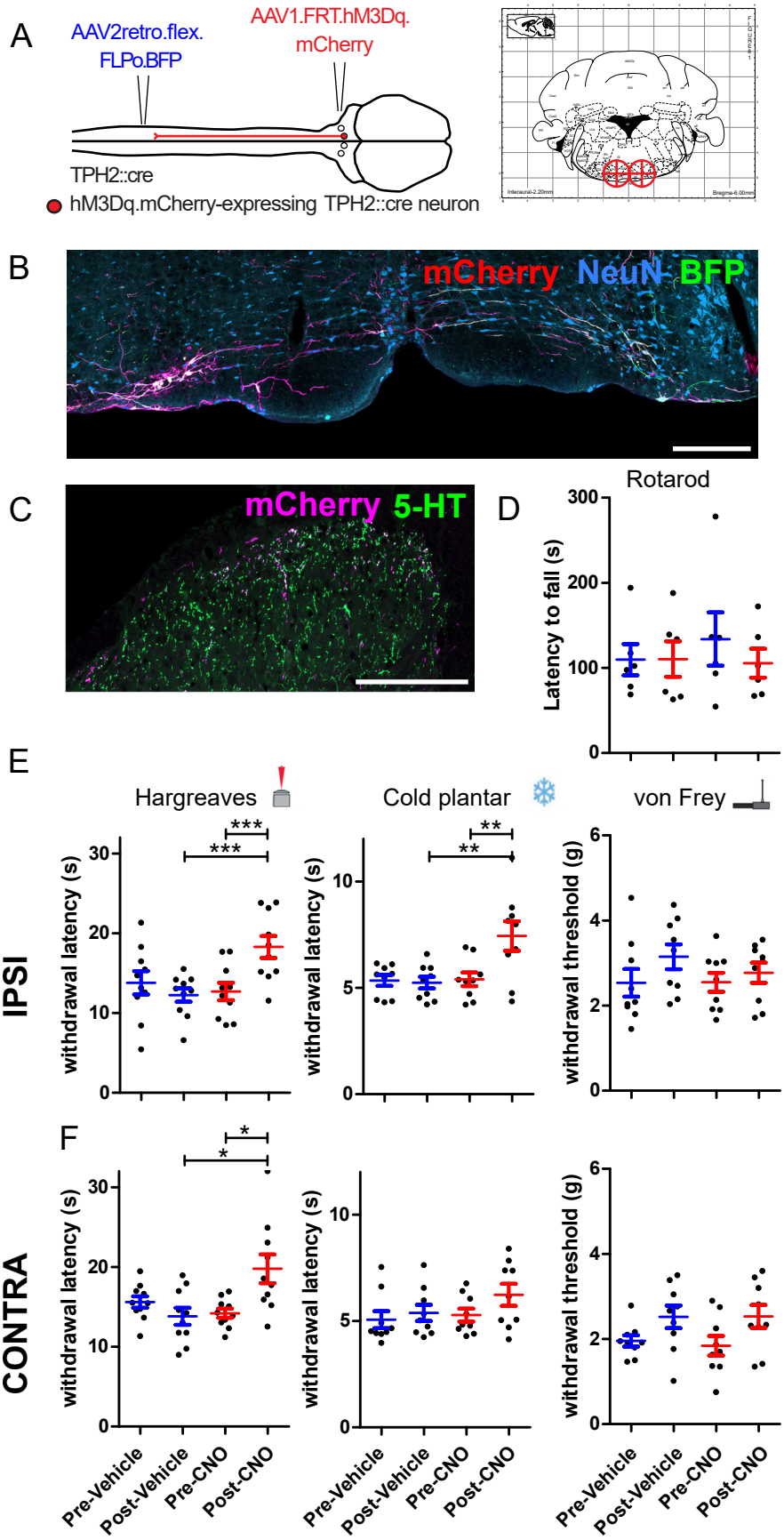
A
AAV2retro.flex.
FLPo.BFP
AAV1.FRT.hM3Dq.
mCherry
TPH2::cre
hM3Dq.mCherry-expressing TPH2::cre neuron
B
mCherry NeuN BFP
C
mCherry 5-HT
D
Rotarod
Latency to fall (s)
E
Hargreaves
Cold plantar
von Frey
IPSI
withdrawal latency (s)
withdrawal threshold (g)
F
CONTRA
Pre-Vehicle
Post-Vehicle
Pre-CNO
Post-CNO

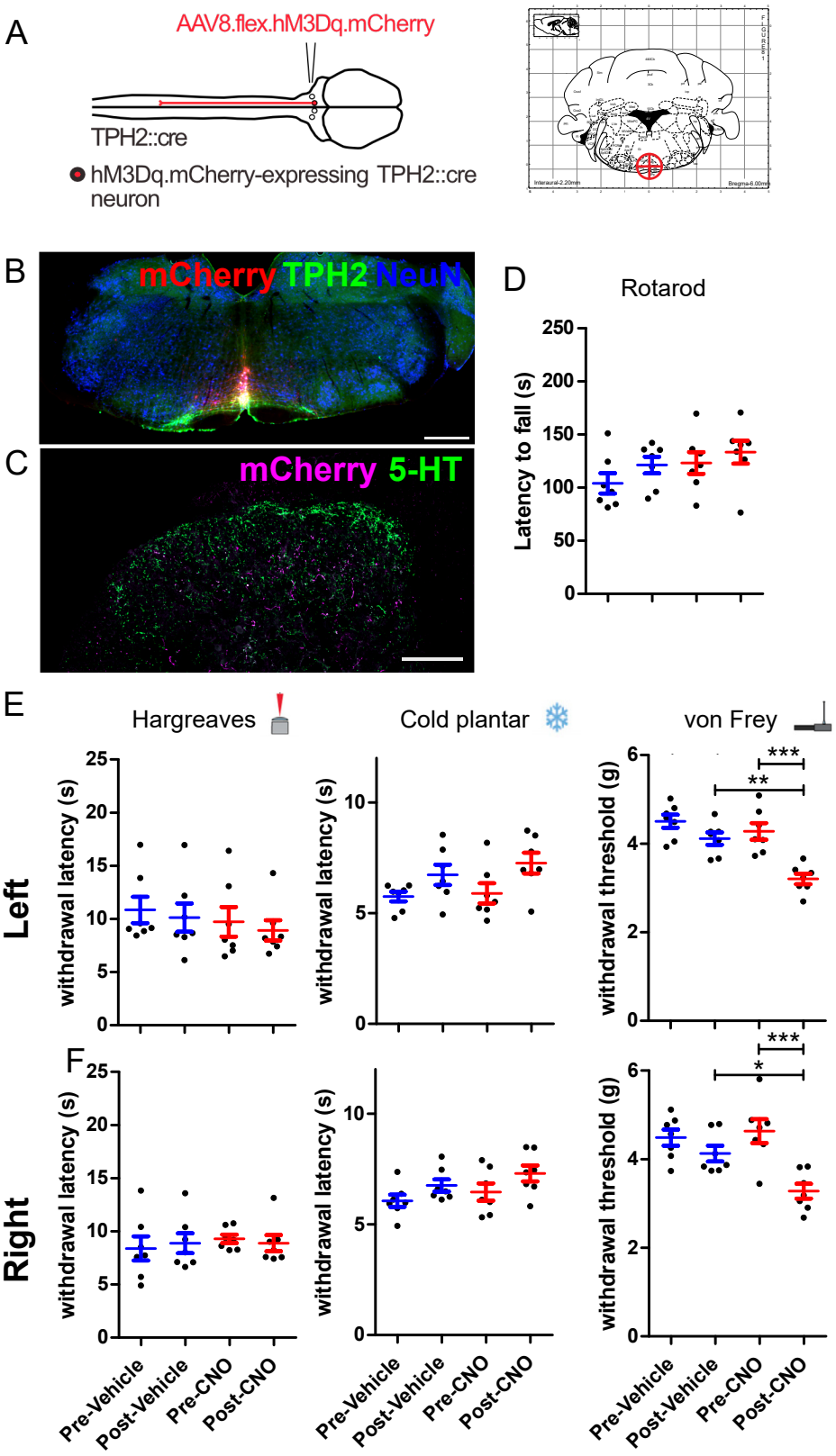
A
AAV8.flex.hM3Dq.mCherry
TPH2::cre
hM3Dq.mCherry-expressing TPH2::cre neuron
B
mCherry TPH2 NeuN
C
mCherry 5-HT
D
Rotarod
Latency to fall (s)
E
Hargreaves
Cold plantar
von Frey
Left
withdrawal latency (s)
withdrawal threshold (g)
F
Right
Pre-Vehicle
Post-Vehicle
Pre-CNO
Post-CNO

Mouse line	Supplier/source	Reference
TPH2::cre	The Jackson Laboratory	MGI: 5435520
Hoxb8-cre	Pawel Pelczar	(Witschi et al. 2010)
ROSA26^{TVA}	Dieter Sauer	(Seidler et al. 2008)

Table 1: Transgenic mouse lines used in this study

Seidler, B., A. Schmidt, U. Mayr, H. Nakhai, R. M. Schmid, G. Schneider & D. Saur (2008) A Cre-loxP-based mouse model for conditional somatic gene expression and knockdown in vivo by using avian retroviral vectors. *Proc Natl Acad Sci U S A,* 105**,** 10137-42.

Witschi, R., T. Johansson, G. Morscher, L. Scheurer, J. Deschamps & H. U. Zeilhofer (2010) Hoxb8-Cre mice: A tool for brain-sparing conditional gene deletion. *Genesis,* 48**,** 596-602.

Reagent	Supplier/Source	Cat#/RRID
Cholera toxin b subunit	Sigma Aldrich	C9903-.5MG/
Fluorogold	Biotium	BIO80014

Table 2: Non-viral retrograde tracers used in the study

Virus name	Full name	Supplier/Source	Cat#
AAV2retro.eGFP	ssAAV-retro/2-CAG-EGFP-WPRE-SV40p(A)	Viral Vector facility UZH/ETHZ	V24-retro
AAV2retro.flex.eGFP	ssAAV-retro/2-shortCAG-dlox-EGFP(rev)-dlox-WPRE-SV40p(A)	Viral Vector facility UZH/ETHZ	V158-retro
AAV2retro.flex.FLPo.BFP	ssAAV-retro/2-hSyn1-chI-dlox-EBFP2_2A_FLPo(rev)-dlox-WPRE-SV40p(A)	Viral Vector facility UZH/ETHZ	V175-retro
AAV2retro.flex.FLPo.mCherry	ssAAV-retro/2-hSyn1-chI-mCherry_2A_FLPo-WPRE-SV40p(A)	Viral Vector facility UZH/ETHZ	V173-retro
AAV8.flex.eGFP	ssAAV-8/2-hSyn1-dlox-EGFP(rev)-dlox-WPRE-hGHp(A)	Viral Vector facility UZH/ETHZ	V115-8

AAV8.flex.tdTomato	ssAAV-8/2-hSyn1-dlox-tdTomato(rev)-dlox-WPRE-bGHp(A)	Viral Vector facility UZH/ETHZ	v284-8
AAV9.flex.tdTomato	ssAAV-9/2-hSyn1-dlox-tdTomato(rev)-dlox-WPRE-bGHp(A)	Viral Vector facility UZH/ETHZ	v284-9
AAV8.flex.hM3Dq.mCherry	ssAAV-8/2-hsyn1-dlox-hM3D(Gq)_mCherry(rev)-dlox-WPRE-hGHp(A)	Viral Vector facility UZH/ETHZ	v89-8
AAV9.FRT.eGFP	ssAAV-9/2-hSyn1-chI-dFRT-EGFP(rev)-dFRT-WPRE-hGHp(A)	Viral Vector facility UZH/ETHZ	V335-9
AAV1.FRT.hM3D(q).mCherry	ssAAV-1-hSyn1-dFRT-hM3D(Gq)-mCherry	Viral Vector facility UZH/ETHZ	V189-1
SAD pseudotyped rabies	SAD.RabiesΔG-eGFP (SAD-G)	Karl-Klaus Conzelmann	N/A
EnvA pseudotyped rabies	SAD.RabiesΔG-GFP (EnvA)	Karen Haenraets	N/A

Table 3: AAVs and rabies viruses used in the study

Antibody	Host	Supplier/Source	Cat#/RRID	Dilution
GFP	Chicken	LifeTech	A10262/ AB_2619988	1:1000
TPH2	Rabbit	Novus Biologicals	NB100-74555/AB_572263	1:1000
Ctb	Goat	LIST biological laboratories inc.	#703/AB_2314252	1:1000
mCherry	Goat	Sicgen	AB0081-200/AB_2333094	1:500
tdTomato	Goat	Sicgen	AB8181-200/ AB_2722750	1:500
5-HT	Rabbit	ImmunoStar	20080/AB_572263	1:1000
NeuN	Guinea pig	Synaptic systems	266004/AB_2619988	1:1000
Chicken-Alexa 488	Donkey	Jackson ImmunoResearch	703-546-155/AB_2340376	1:500
Goat-Cy3	Donkey	Jackson ImmunoResearch	705-166-147/AB_2340413	1:500
Goat-Alexa 488	Donkey	Jackson ImmunoResearch	795-546-147/ -	1:500

Guinea pig-Alexa 647	Donkey	Jackson ImmunoResearch	706-496-148/ -	1:500
Rabbit-Alexa 647	Donkey	Jackson ImmunoResearch	711-607-003/AB_2340626	1:500
Rabbit-Cy3	Donkey	Jackson ImmunoResearch	711-165-152/AB_2307443	1:500

Table 4: antibodies used in the study

labelling strategy	rabies virus	animals	total GFP+ cells counted in RVM	GFP neurons expressing TPH2	GFP neurons expressing TPH2	% GFP+ neurons that are TPH2+
direct infection (5d)	SAD.RabiesΔG-eGFP (SAD-G)	3	25 (5-11)	11 (2-5)	14 (3-6)	44 (40-45)
direct infection (7d)	SAD.RabiesΔG-eGFP (SAD-G)	3	36 (7-17)	4 (1-2)	32 (6-16)	11 (6-16)
monosynaptic tracing	SAD.RabiesΔG-eGFP (EnvA)	4	33 (3-20)	1 (0-1)	32 (3-19)	3 (0-5)

Table 5: Neurons in the ventral hindbrain traced from the spinal cord with modified rabies viruses. Number represents the total number of cells counted with the range of cells counted for each animal in parentheses. Percentages of labelled neurons expressing TPH2 are the average for all cells counted per group, with the range for each animal given in parentheses.

Brain region	Subset	GFP only	Ctb only	GFP+Ctb+	%GFP only	%Ctb only	%GFP+Ctb+
RVM (all neurons)	-	99 (11 - 57)	679 (149 – 319)	279 (65 – 134)	9.1 (4.0 – 12.1)	65.6 (59.7 – 73.3)	25.3 (22.7 – 28.1)
RVM (TPH2+ neurons)	All	5 (0 – 4)	269 (63 – 123)	62 (12 – 25)	1.5 (0 – 5.1)	80.1 (76.1 – 83.1)	18.5 (15.2 – 22.9)
	LPGi	5 (0 – 4)	79 (16 – 44)	35 (7 – 15)	4.2 (0 – 14.8)	66.4 (54.3 – 77.2)	29.4 (22.8 – 42.9)
	NRM	0 (0 – 0)	143 (37 – 63)	15 (4 -6)	0 (0 – 0)	90.5 (87.8 – 94.0)	9.5 (6.0 – 12.2)
	Other	0 (0 – 0)	47 (10 – 21)	12 (0 – 8)	0 (0 – 0)	79.7 (66.7 – 100)	20.3 (0 – 33.3)

Table 6: Quantification of hindbrain neurons traced from the spinal dorsal horn with AAV2retro.eGFP and CTb The number in each column is the total number of cells counted for each group, with the range of cells counted for each animal in parentheses. For percentages, the average value is presented with the range for each animal given in parentheses.

Parameter	NRM	LPGi
Membrane resistance (MΩ)	1643 ± 240.1	1857 ± 316.9
Resting membrane potential (mV)	-64.69 ± 4.145	-70.32 ± 3.592
Rheobase current (pA)	18.75 ± 2.236	15.00 ± 2.266
Action potential threshold (mV)	-32.45 ± 2.597	-34.18 ± 0.8890
Action potential amplitude (mV)	85.26 ± 3.230	79.14 ± 4.194
Action potential half width (ms)	1.730 ± 0.1960	1.875 ± 0.2198
Slow Afterhyperpolarisation (with AHP / total)	9/10	5/8
Slow Afterhyperpolarisation Amplitude (mV)	27.09 ± 0.7983	27.58 ± 1.304

Table 7: Comparison of active and passive membrane properties between serotonergic neurons in the NRM and the LPGi. Data are shown as mean ± SEM (n = 10 NRM, n= 8 LPGi)